DNA Alkylation Repair Deficient Mice Are Susceptible To Chemically Induced Inflammatory Bowel Disease

by

Stephanie Lauren Green

B.S. Mechanical Engineering
Carnegie Mellon University, 2003

SUBMITTED TO THE DEPARTMENT OF BIOLOGICAL ENGINEERING IN PARTIAL FULFILLMENT OF THE REQUIREMENTS FOR THE DEGREE OF

MASTER OF SCIENCE IN BIOLOGICAL ENGINEERING
AT THE
MASSACHUSETTS INSTITUTE OF TECHNOLOGY

FEBRUARY 2006

Signature of Author: _____
Department of Biological Engineering
January 20, 2006

Certified by: _____
Leona D. Samson
Professor of Biological Engineering
Thesis Supervisor

Accepted by: _____
Alan J. Grodzinsky
Professor of Biological Engineering
Chair, Biological Engineering Graduate Program Committee

DNA Alkylation Repair Deficient Mice Are Susceptible To Chemically Induced Inflammatory Bowel Disease

by Stephanie Lauren Green

Submitted to the Department of Biological Engineering on January 20, 2006 in Partial Fulfillment of the Requirements for the Degree of Master of Science in Biological Engineering

Abstract

The two most common forms of inflammatory bowel disease (IBD) are ulcerative colitis (UC) and Crohn's Disease (CD), which affect more than 1 million Americans. Recently the incidence of IBD has been rising in Japan, Europe and North America.[1] Colorectal cancer is a very serious complication of IBD, and a patient's risk increases with increasing extent and duration of disease.[2] There is no cure for CD, and the only cure for UC is removal of the entire colon and rectum. It is thought that cancer risk is based on chronic inflammation of the gastrointestinal mucosa. There have been many studies, which have supported this idea and have made progress toward understanding the link between chronic inflammation and cancer. In both UC and CD, it is known that there are increased levels of εA, εG, and εC, which are potentially miscoding lesions, in the DNA of affected tissues.[3] Also, 3-methyladenine DNA glycosylase (*Aag* in mice), an initiator of the Base Excision Repair pathway, shows adaptively increasing activity in response to increased inflammation in UC colon epithelium.[4]

This thesis demonstrates the importance of *Aag* in protecting against the effects of chronic inflammation. It was found that *Aag* deficient mice, treated with 5 cycles of dextran sulfate sodium (DSS) to induce chronic inflammation, showed significant signs of increased disease including decreased colon length, increased spleen weight, and increase in epithelial defects. Also, when treated with a tumor initiator, azoxymethane, prior to DSS exposure, *Aag* deficient mice show a 2.95 fold ($p<0.0001$) increase in tumor multiplicity compared to wild type treated animals, as well as decreased colon length, increased spleen weight, increased dysplasia/neoplasia, and increased area affected by dysplasia/neoplasia.

If UC patients had a deficiency in 3-methyladenine-DNA-glycosylase activity, they would likely be more susceptible to mutations and cancer because of their inability to repair DNA damage caused by inflammatory cytokines and reactive oxygen and nitrogen species. In future studies, it would be beneficial to determine if transgenic *Aag* over-expresser mice show protection against the damage induced by chronic inflammation. This would make intestinal gene therapy a possible approach to finding the first cure for IBD and inflammation associated colorectal cancer.

Thesis supervisor: Leona D. Samson
Title: Professor of Biological Engineering

Acknowledgements

I would like to thank my advisor, Professor Leona Samson, for giving me the opportunity to work on this project, and also for all of her encouragement and support during my time in the lab. I would also like to thank Professor Samson for being a great role model for me in pursuing a scientific career and for her enthusiasm in the pursuit of knowledge. In addition, I would like to thank Dr. Lisiane Meira for all of her guidance and for the many hours spent teaching me useful lab techniques and doing mouse dissections. She has been constantly supportive during my time at MIT. Jamie Bugni was also a great help in teaching me processing of mouse intestines and in having insightful project discussions. Lab technicians Catherine Moroski and Kristin Daigle greatly supported me both in and out of the lab, and helped a lot in the mouse room and with dissections. All of the members of the Samson Lab have been great to work with and were always eager to help me in the lab. This project was funded through two sources. I would like to thank the Medtronic Foundation for the Medtronic Graduate Fellowship which supported me during my first year and also the NIH for support me through grant #5-R01-CA075576-08 during the last year and a half. I truly appreciate their generosity. Finally, I would like to thank my parents for teaching me the value of education, my husband for his unconditional love and support and for feedback and scientific discussions, and especially my brother for inspiring me to work on this project.

Table of Contents

List of Figures

List of Tables

List of Abbreviations

AAG, Aag	alkyladenine glycosylase, 3-methyladenine DNA glycosylase
$Aag^{-/-}$	*Aag* null
APC	Adenomatous polyposis coli
AP	apurinic/apyrimidinic
CD	Crohn's Disease
CYP2E1	Cytochrome P450 2E1
ε	Etheno
EGF	Epidermal growth factor
ER	Endoplasmic reticulum
IBD	Inflammatory bowel disease
ICR	Crj: CD-1 mouse strain from Charles River Japan
IKK	IκB kinase
IL	Interleukin
LPO	Lipid peroxidation
PBS	Phosphate buffered saline
RONS	Reactive Oxygen and Nitrogen Species
TNF	Tumor necrosis factor
TGF	Transforming growth factor
UC	Ulcerative colitis

Chapter 1: Introduction

1.1 Inflammatory Bowel Disease

Inflammatory bowel disease (IBD) is any inflammatory disease of the gastrointestinal tract. IBD can develop from a number of factors including immune system, heredity, and environment.[7] When the body's immune system tries to fight off an invading virus or bacteria, the digestive tract becomes inflamed due to the immune response. Also, direct infection of hematopoietic and epithelial cells by the virus or bacteria can induce mutations in tumor suppressors and proto-oncogenes, or can alter signaling pathways which lead to cell proliferation or survival through extracellular factors.[8] The two most common forms of IBD are ulcerative colitis (UC) and Crohn's Disease (CD) and affect more than 1 million Americans. About twenty percent of people with UC or Crohn's disease have a parent, sibling, or child who also has the disease, but a responsible gene has not yet been discovered.[7] IBD has also been found to occur more often among people living in cities and industrial nations. It is possible that environmental factors, such as high fat diets or refined foods, may play a role in the development of IBD since there is such a vast difference in incidence worldwide.[1] Recently the incidence of IBD has been rising in Japan, Europe and North America.[1]

There are many detrimental side effects of IBD which can affect a patient's quality of life. Arthritis afflicts about 25 percent of patients, high levels of toxins that result from IBD cause serious liver disease in 3 to 7 percent of patients, weight loss is seen in 65 to 75 percent of patients, and continual decline in food intake can result in malnutrition and

is the most common reason IBD patients require hospitalization.[7] Colorectal cancer is also a very serious complication of IBD, and a patient's risk increases with increasing extent and duration of disease.[2] In the 19th century, Rudolf Virchow demonstrated the presence of leukocytes in malignant tissues and claimed that tumors develop from areas of chronic inflammation.[8] Recently, there was found to be an 18-fold increase in risk of colorectal cancer in patients with extensive CD and 19-fold increase in risk for patients with extensive UC as compared to the general population.[9] As a genetic basis is yet to be identified as an indicator of predisposition to colorectal cancer, it is thought that cancer risk is likely based on chronic inflammation of the gastrointestinal mucosa.[5] There have been many studies, which have supported this idea and have made progress toward understanding the link between chronic inflammation and cancer.

1.1.1 Crohn's Disease and Ulcerative Colitis

An estimated 500,000 Americans have Crohn's disease, which usually affects the lower part of the small intestine (ileum) or colon, but can flare up anywhere in the digestive tract from the mouth to anus.[7] It can also spread deep into the layers of affected tissue and inflamed regions may include large ulcers separated by patches of healthy tissue. There is no cure for CD and current medications are aimed at decreasing inflammation and alleviating symptoms. Approximately one in four adults with Crohn's disease develops fistulas or abscesses. Many people require surgical resection due to complications such as blockage, abscess, perforation or bleeding in the intestines.

Unlike CD, UC only affects the innermost lining (mucosa) of the colon and rectum. The affected areas are continuous and may contain small bleeding ulcers. UC affects men and women equally and appears to run in some families, most often occurring between the ages of fifteen and forty.[7] Patients can develop side effects such as severe arthritis, liver disease, kidney stones, gallstones and mouth ulcers that prohibit swallowing or eating. Like CD, current therapies for UC target inflammation or aim to alleviate symptoms. Patients with chronic UC often go through recurrence and remission cycles.[10] During an inflammation phase, the patient develops mucosal ulceration along with necrosis, while during remission there is regeneration of the colonic mucosa.[10] Increases in cell proliferation and cell death are characteristic of active phase UC.[10] About 25-40% of patients have their colon removed by Ileal-anal pouch surgery because of massive bleeding, severe illness, rupture of the colon, or risk of cancer. Approximately 5% of UC patients develop colon cancer, although it is probable that this percentage would be even higher if such a large number of patients did not have surgery.

1.1.2 Current Treatments

Anti-inflammatory drugs are often the first step in the treating IBD and are used to relieve signs and symptoms. Immune system suppressors can also reduce inflammation, but target the immune system rather than treating inflammation itself. The fact that these drugs are often effective in treating IBD and may prevent the development of cancer, supports the idea that damage to digestive tissues is caused by the body's immune response.[5] Antibiotics generally have no effect on UC, but can be used to heal fistulas

and abscesses in people with Crohn's disease. Interestingly, it has been found that nicotine patches can give short-term relief from flare-ups of UC and appear to eliminate symptoms in four out of 10 people.[7] Other medications such as anti-diarrheals, laxatives, pain relievers, iron supplements, and vitamin B-12 injections (to prevent anemia), are also used to relieve signs and symptoms of the disease. Currently, surgery is the only cure for UC and is often the best option for CD, even though it can only buy years of remission at best. Surgery usually means removal of the entire colon and rectum (proctocolectomy) for UC and removal of diseased sections of intestine (colonic resection) for CD.

1.1.3 Disease Progression and Colon Cancer

During a flare up in humans, indications of increased disease include decrease in body weight, blood in stool, stool consistency, iron deficiency, raised white cell count, low serum albumin due to protein loss from inflamed intestine and impairment of liver function, severity of colon inflammation and formation of polyps.[11] In mice indicators also include increase in spleen weight, decrease in colon length, and increased colon weight per length. It is thought that inflammation leads to epithelial-derived tumors, and the processes which link epithelial and inflammatory cells during inflammation-associated tumor development is currently being studied by many groups.[8]

As a result of damage, ulcers can form and hyperproliferation can lead to hyperplasia and early tumors, or small polyps. These polyps or adenomas then grow until they invade the

basement membrane of the colon becoming adenocarcinomas and then metastasize, entering the blood stream and spreading to other tissues in the body as shown in Figure 1.

Even before there is histological evidence of dysplasia or cancer, chromosomal instability, microsatellite instability, and p16 (cell cycle inhibitor) promoter hypermethylation are all seen in regions of intestine affected by colitis as described by Figure 2.[5] Loss of adenomatous polyposis coli (APC), a tumor-suppressor gene, is an early event in sporadic colon cancer (as shown in Figure 1), however, in colitis-associated colon cancer, it is rarely seen until later stages of disease in areas with definite dysplasia (shown in Figure 2). In IBD patients, dysplasia can be polypoid or flat, localized, diffuse, or multifocal, and any dysplasia at all indicates increased risk of neoplasia in the entire colon.[5] It is therefore common practice to remove the entire colon and rectum rather than sections in UC.

Since IBD cases vary among patients, it is difficult to monitor for cancer and makes it very important to understand how chronic inflammation contributes to cancer development. After 7 years of colitis, risk of colorectal cancer increases at a rate of 0.5-1.0% per year.[5] Also, greater extent of colitis and degrees of histologically active inflammation are associated with greater risk of colonic neoplasia.[5, 12]

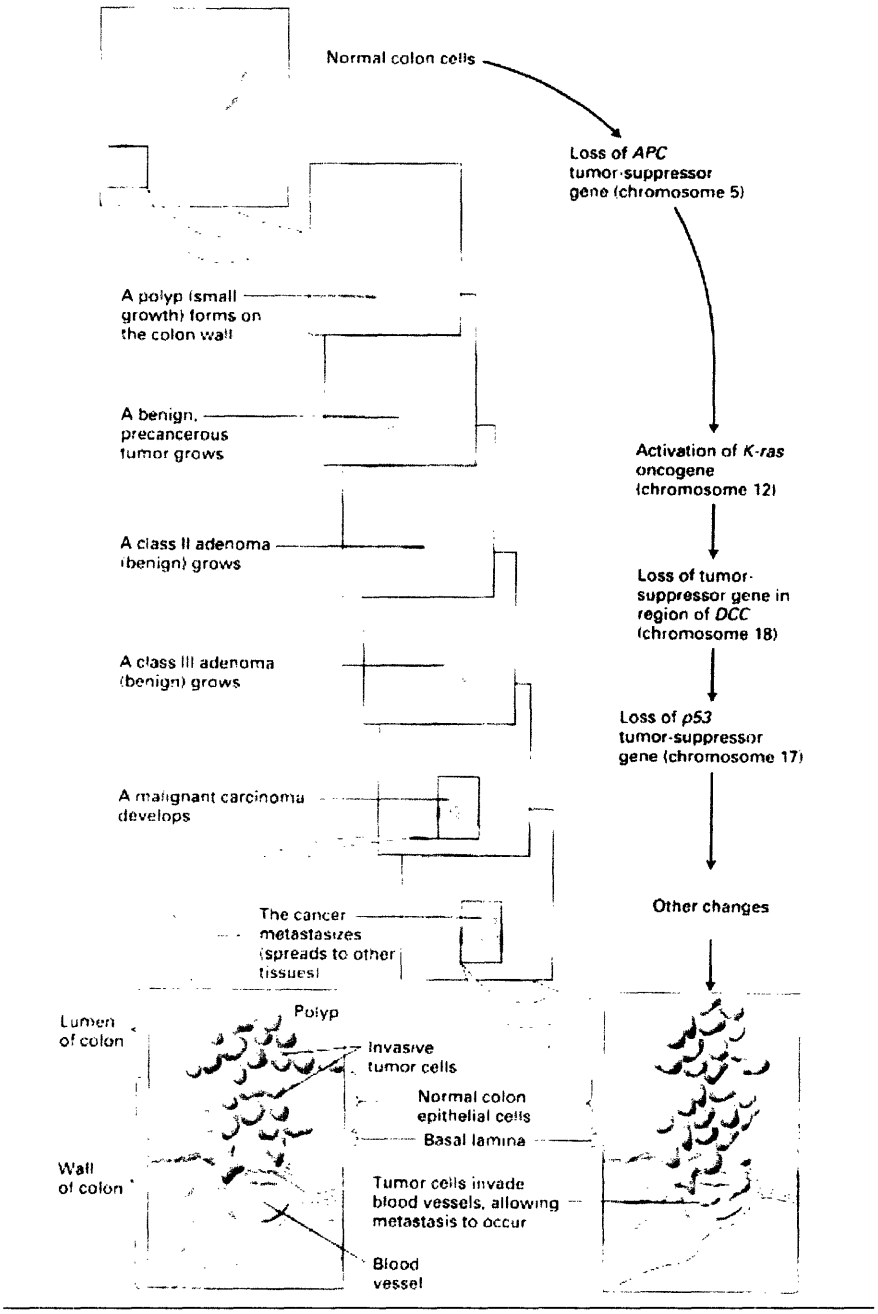

Figure 1. Damage to DNA can cause hyperproliferation and inhibit apoptosis, leading to the development of polyps which can grow into adenomas and eventually carcinomas. Carcinomas can metastasize and spread throughout the body causing cancer in other organs or tissues.[13] (Figure taken from Molecular Cell Biology, Lodish et al.)

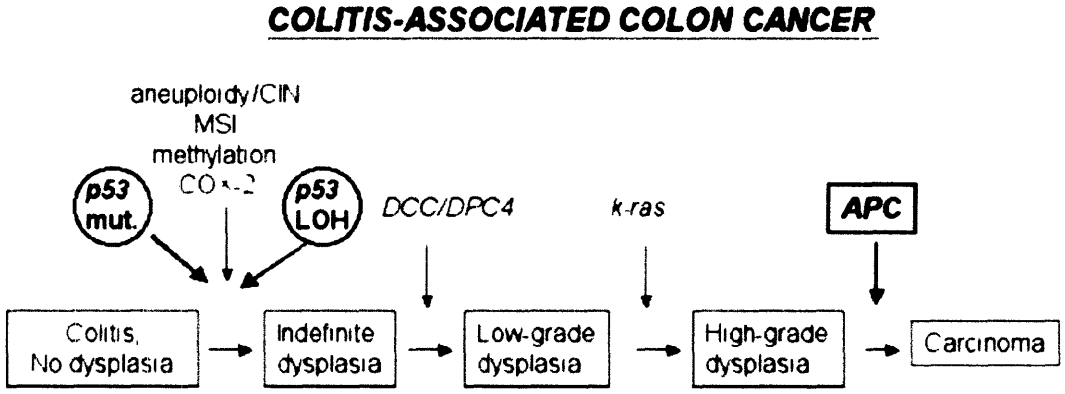

Figure 2. Chromosomal instability, microsatellite instability, and hypermethylation are all seen in regions of intestine affected by colitis. P53 mutations are an early event in colitis associated colorectal cancer.[5] (Figure taken from Inflammation and Cancer IV. Colorectal cancer in inflammatory bowel disease: the role of inflammation, Itzkowitz et al.)

1.1.4 The need for further understanding and better treatments

As previously mentioned, there is no cure for CD, and the only cure for UC is removal of the entire colon and rectum. The severity of these diseases calls for a much better understanding of their initiation, development, and treatment. Many studies have elucidated some of the pathways and key players involved in early and late stages of IBD, although there is no clear mechanism of progression as of yet.

Using DNA aneuploidy as a marker, individual cell populations were seen to become more widely distributed over time using repeated colonoscopies.[5] Aneuploidy is often more widespread than dysplasia, so genomic alterations can be taking place in the colonic

mucosa without any change in morphology.[5] In colitis, p53 mutations occur early, even without dysplasia, in the inflamed mucosa of patients, which suggests that chronic inflammation predisposes them to early mutations. Alteration of p53 is also an early event in UC associated neoplasia.[14] Loss of $p14^{ARF}$ function, an indirect regulator of p53, has been seen in 60% of mucosal samples from UC patients without dysplasia.[5]

It has also been shown that there is translocation of β-Catenin from the cell membrane in untransformed epithelium to the cytoplasm or nucleus in human UC associated neoplasia.[2, 8, 14] β-Catenin is part of the Wnt-APC signal transduction system, and its nuclear accumulation can be a result of mutations in APC, β-Catenin, or Axin (a mediator of β-Catenin phosphorylation).[2] This transformation of β-Catenin has negative effects when nuclear accumulation occurs, since β-Catenin regulates transcription of genes that can affect growth and cell differentiation.[2] Also contributing to unregulated growth is TNF-α, a proinflammatory cytokine that is involved in tumor progression in human intestinal mucosa through initiation and promotion of neoplasia.[2, 15]

Nf-κB is a transcription factor which is activated in response to infectious agents and proinflammatory cytokines through the IκB kinase (IKK) complex. IκB inhibits Nf-κB dimers from leaving the cytoplasm. Microbial and viral infections and proinflammatory cytokines activate the IKK complex. IKK then phosphorylates the IκBs, targeting them for ubiquitin-dependent degradation and freeing Nf-κB dimers which can then enter the nucleus. Nf-κB is known to activate genes whose products inhibit apoptosis and its constitutive activation was suggested to contribute to cancer.[8]

Deletion of IKKβ in intestinal epithelial cells does not decrease inflammation, as detected histologically and through mRNA levels of proinflammatory proteins, but dramatically decreases tumor incidence without affecting tumor size.[8] Deletion of IKKβ in myeloid cells results in a significant decrease in tumor size and diminishes expression of proinflammatory cytokines that may act as tumor growth factors, without affecting apoptosis.[8] Immune cells secrete proinflammatory cytokines, such as TNF-α, IL-1, IL-6, and IL-8, and also matrix-degrading enzymes, growth factors, and reactive oxygen species (RONS). Such an extracellular environment promotes tumor development by leading to cell proliferation, cell survival, cell migration, and angiogenesis.[8]

It is also known that iNOS is induced in inflamed regions of human colonic epithelium and has been suggested that iNOS leads to the production of nitric oxide, which interacts with superoxide to produce peroxynitrite, which reacts with tyrosine to form nitrotyrosine in cellular proteins.[16] RONS are known to be secreted by inflammatory cells and are also known to cause many forms of damage.

All of these molecules are involved in inflammation and cancer, but the role of DNA repair in this process has not yet been well studied. It is possible that small changes to DNA bases, such as alkylation damage, can have an effect as well as larger DNA alterations such as aneuploidy. It is known that inflammation leads to the production of RONS, which create substrates for 3-methyladenine DNA glycosylase and activation of the base excision DNA repair pathway.

1.2 Inflammation, Reactive Oxygen and Nitrogen Species, and DNA Damage

1.2.1 RONS

At a site of inflammation, phagocytes synthesize large amounts of RONS, which accumulate in the mucosa and can damage lipids, proteins, and DNA. RONS can also react with fatty acid chains leaving radicals that can eventually react with each other to form covalently crosslinked side chains. Crosslinked membrane lipids may become so deformed that they damage the membrane. In addition, RONS can cause structural alterations in DNA (point mutations, rearrangement, insertions, deletions), gross chromosomal alterations (loss of a second wild type allele of mutated proto-oncogene or tumor-suppressor gene), and affect cytoplasmic and nuclear signal transduction (activation of transcription factors).[17] They can also modulate activity of proteins and genes that respond to stress and regulate cell proliferation, differentiation, and apoptosis. During the chronic inflammatory processes an excess of free radicals and DNA-reactive aldehydes from lipid peroxidation (LPO) are produced, which deregulate cellular homeostasis and can drive normal cells to malignancy. Etheno (ε)-modified DNA bases are generated by reactions of DNA with a major LPO product, trans-4-hydroxy-2-nonenal. It has been shown that there is an increase in lipid peroxides in rectal biopsy samples from patients with active UC, which is consistent with damage by RONS.[17] Figure 3 shows a scheme of RONS and how they can lead to many types of DNA damage.

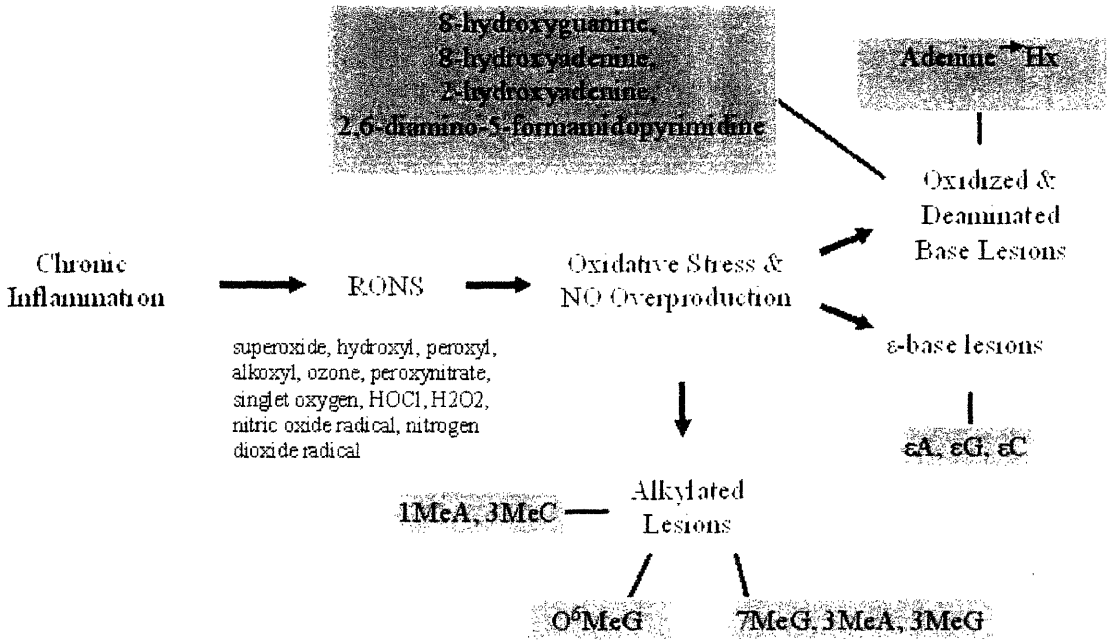

Figure 3. Chronic inflammation leads to overproduction of RONS, which generate DNA damage. Blue boxes indicate various adducts or modified DNA bases that are formed.

In both forms of IBD there are increased levels of εA, εG, εC in the DNA of affected tissues.[3] Also, it has been shown that 3-methyladenine DNA glycosylase (*AAG* in human), which initiates repair of some of these lesions and many lesions generated by RONS, shows adaptively increasing activity in response to increasing inflammation in UC colon epithelium.[4] This suggests that the rise in damaged DNA bases is due to increased oxidative damage rather than decreased repair activity. It is also known that RONS can induce O^6MeG, which is a substrate for O^6-methylguanine DNA methyltransferase (*MGMT*), a protein that acts in direct reversal of base damage. Accumulation of unrepaired DNA damage can lead to mutations and cancer. The link

between oxidative stress, lipid peroxidation, DNA damage, and cancer is extremely important, and *AAG* and *MGMT* may be key players in the process, which must be further studied.

1.2.2 DNA Damage Repair by Base Excision Repair Pathway

As mentioned above, *AAG* may be a very important factor in the development of colitis-associated colorectal cancer. Accelerated epithelial cell turnover caused by chronic inflammation and epithelial damage might predispose the mucosa to DNA damage.[10] DNA repair mechanisms target this damage and are important in maintaining correct genomic structures.[6] A pathway involved in repairing many of the lesions generated by RONS is the Base Excision Repair (BER) pathway, initiated by one of the many different DNA glycosylases, namely the 3-methyladenine DNA glycosylase. In humans, this glycosylase is named AAG and in mice it is referred to as Aag. These glycosylases repair a large range of substrates including 3-MeA, 7-methylguanine, 3-methylguanine, hypoxanthine, 1,N^6-ethenoadenine, N^2,3-ethenoguanine and possibly 8-oxoguanine in humans. Human 3-methyladenine DNA glycosylase can also remove normal guanines, but with very low efficiency.[6] Figure 4 shows a diagram of the BER pathway.

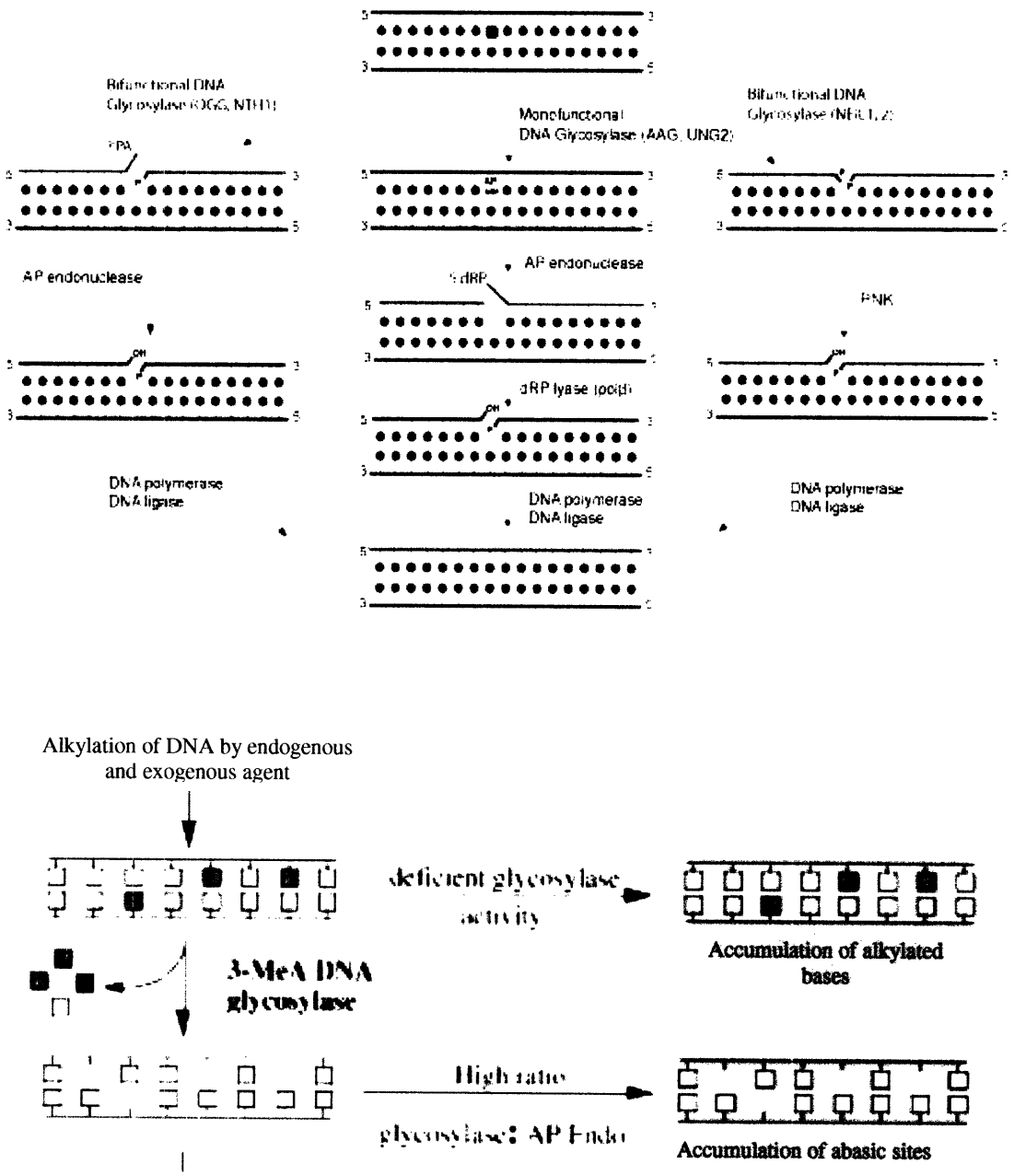

Figure 4. The BER pathway can be initiated by 3-methyladenine DNA glycosylase and repairs many unwanted DNA lesions. An imbalance in glycosylase activity can cause accumulation of abasic sites and further damage. (Figures from 3-Methyladenine DNA glycosylases: structure, function, and biological importance, Wyatt et al.)[6]

BER is initiated by DNA glycosylases, which cleave the N-glycosylic bond between the damaged base and the deoxyribose leaving an abasic site. In the major pathway of BER, a strand break is made at the abasic site by a 5'-apurinic/apyrimidinic (AP) endonuclease. The abasic end is removed by deoxyribophosphatase or diesterase activity, and the gap is filled by DNA polymerase β. The strand break is finally sealed by DNA ligase III.[6]

As previously stated, it has been shown that UC patients have increasing AAG activity with increasing colonic inflammation. This may indicate a need for more repair, however, an excess of AAG can cause more damage by creating a large number of abasic sites.[6] 3-methyladenine DNA glycosylases may protect against mutagens and cytotoxicity due to environmental or chemical agents by removing alkylated bases or may have detrimental effects by leaving too many abasic sites (Figure 4).[6] It is important to investigate whether or not this glycosylase can protect against or enhance the effects of chronic inflammation. If a UC patient had a deficiency in 3-methyladenine-DNA-glycosylase activity, they may be more susceptible to mutations and cancer if they are unable to repair DNA damage caused by inflammatory cytokines and RONS. However, an imbalance in the BER pathway, causing an excess of AAG activity might also lead to mutations and cancer.

3-methyladenine-DNA-glycosylase has the ability to rescue E. coli from MMS treatment. On the other hand, sensitivity was shown when *AAG* expression was induced in CHO cells, which were then treated with MMS or MNNG.[6] Mouse *Aag* has shown three

different phenotypes in three different mouse derived cell lines, but so far no phenotype or whole animal lethality has been shown in *Aag* deficient (-/-) mice.[6]

1.2.3 DNA Damage Repair by Reversal of Base Damage

A second repair mechanism, involving the *MGMT* protein, is reversal of base damage. During repair, the alkyl DNA lesion is irreversibly transferred to an internal cysteine residue of *MGMT* through a suicidal mechanism. Figure 5 illustrates this process.

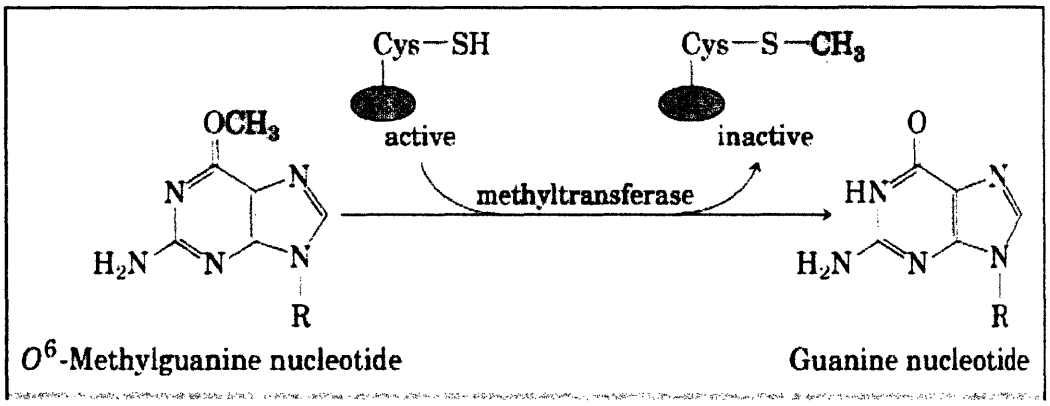

Figure 5. *MGMT* irreversibly transfers alkyl DNA lesions to its internal cysteine residue. (Figure from DNA Repair, M.R. Kelly)[18]

Mgmt knockout (*Mgmt*$^{-/-}$)mice were developed using homologous recombination to delete the active site cysteine.[19] Mouse embryonic fibroblasts and bone marrow cells from these mice show sensitivity to many chemotherapeutic alkylating agents including 1,3-bis(2-chloroethyl)-1-nitrosourea, streptozotocin and temozolomide.[19] Also, unlike *Aag*$^{-/-}$ mice, *Mgmt*$^{-/-}$ mice have shown sensitivity to 1,3-bis(2-chloroethyl)-1-nitrosourea, *N*-methyl-*N*-

nitrosourea, streptozotocin and mitomycin C.[19] When left unrepaired, lesions can lead to mutations and disease. Figure 6 shows how unrepaired O^6MeG lesions cause mispairing with Thymine, and cause damaged bases to propagate.

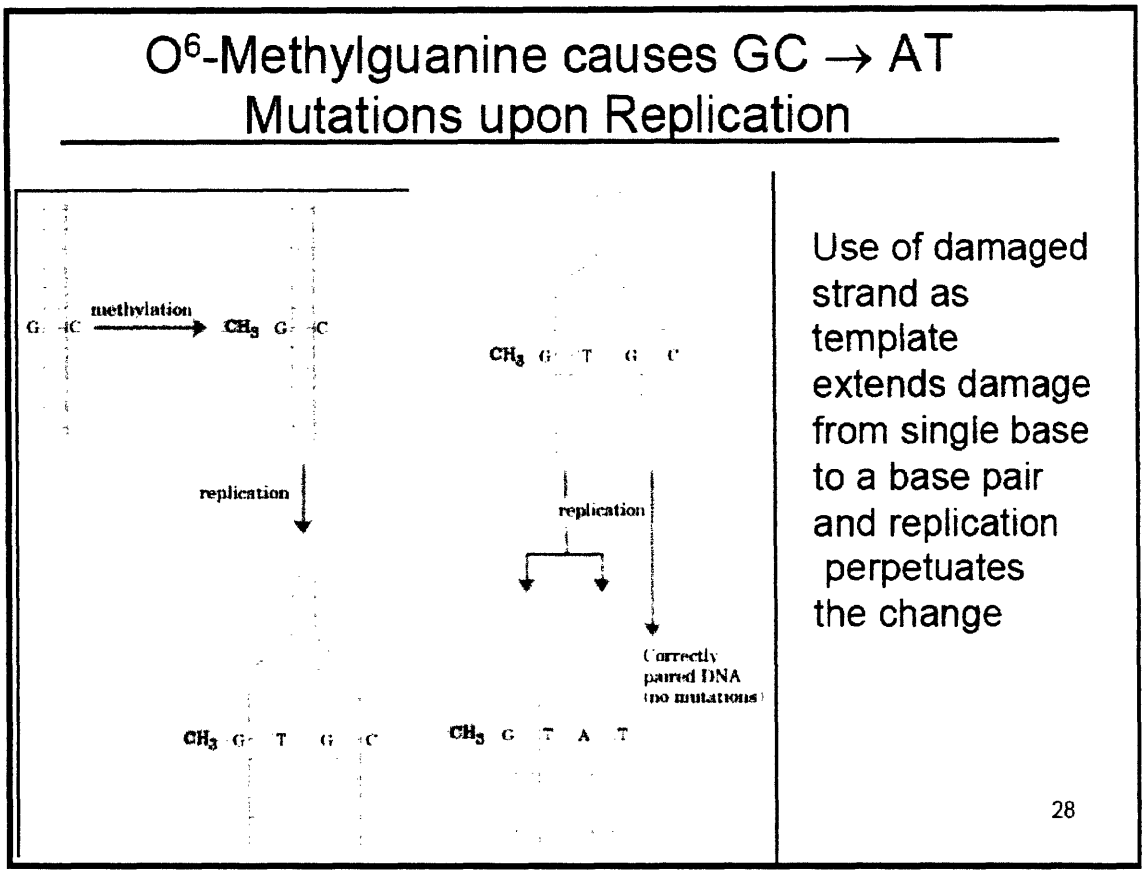

Figure 6. O^6MeG lesions cause mispairing with Thymine, and cause damaged bases to propagate. This can lead to mutations and disease. (Figure from DNA Repair, M.R. Kelly)[18]

1.3 Mouse models of disease

Mouse models are commonly used because of their relevance to human disease. They can give insight into the possible mechanisms of a disease and can closely simulate human response to sicknesses which currently have poor treatment options, such as cancer or inflammatory diseases.[2] Previous studies have shown promising models of chronic IBD. In the Samson Lab, mouse models have been extremely useful in showing the importance of DNA alkylation repair and damage response pathways, as well as studying how DNA repair pathways influence cancer, and sensitivity and resistance to alkylating agents.

The *Aag* null ($Aag^{-/-}$) mouse was developed in the Samson Lab.[20] Embryonic stem cells from the mice were found to be sensitive to alkylating agents.[20] No whole animal phenotype has been shown in response to alkylating agents, and the mice appear healthy. These mice exposed to chronic inflammation can help to predict the BER pathway's contribution in protecting against the effects of IBD.[6]

There are many types of mouse models used to induce IBD in mice including antigen-specific, inducible, genetic, adoptive transfer, and spontaneous models, as described below.

1.3.1 Genetic

These animals include transgenic and knockout models. They can have deficiencies in IL-2, IL-10, T-cell receptor or MHC class-II molecule, TGF-b, and signal transduction molecules. IL-10 deficient mice can be used to study secondary colon cancer which develops in 65% of mice after 30 weeks, although genetic background is very important in severity of colitis.[21] In general, genetic models are very difficult models to study human disease because of variability.

1.3.2 Adoptive Transfer

Adoptive transfer is when T-cells are transferred to genetically identical immunodeficient mice. These mice will then develop colitis, involving the entire large intestine, in about 6 to 8 weeks. Genetic background is important in this model, and although it is highly reproducible and an easy model to develop, the mice have an underlying immunodeficiency, which can complicate the analysis of immune-dependent processes.[21]

1.3.3 Spontaneous

The two spontaneous models which have been described are the SAMP1/Yit and the C3H/HeJBir. The SAMP1/Yit model develops terminal ileitis and has similar features to CD, and the C3H/HeJBir model develops colitis in cecum and right colon at 3 to 4 weeks old.[21] The C3H/HeJBir model does not seem to be as clinically relevant to human UC as

some of the other models. Mice develop transmural inflammation characterized only by a Th1 response.[21] The SAMP1/Yit model is more relevant for CD than UC.

1.3.4 Antigen Specific

Antigen Specific mouse models include the ovalbumin-specific T-cell receptor transgenic model DO11, and models where induction of IBD is caused by Helicobacter hepaticus infection. The DO11 model creates a somewhat artificial in vivo situation and requires the transfer of OVA TCR-tg T cells into immunodeficient mice.[21] Also, inflammation takes several months, so it is difficult to study early events. In the Helicobacter hepaticus model mice develop colitis and secondary adenocarcinoma in IL-10 deficient mice and Rag-2 deficient mice not treated with IL-10.[21] Since IL-10 is secreted during inflammation, it does not seem like this model would be as relevant to human disease.

1.3.5 Inducible

Inducible models in mice include many forms of DSS models and the oxazolone model. The oxazolone model has poor reproducibility and so is not very useful for colitis studies.[21] The DSS models have simple induction, immediate inflammation, and high reproducibility. Although background is important, and non-chronic DSS alone has limited resemblance to IBD, there is much resemblance to human IBD when mice are treated chronically. The next section will go into more detail about the relevance of DSS

models and what has been found in other studies including inflammatory response and tumor incidence.

1.4 AOM/DSS Model of IBD

The DSS/AOM is an inducible model of IBD with immediate inflammation and high reproducibility.[21] Multiple cycles of DSS induce chronic inflammation which is very relevant to human disease. Previous studies have suggested that repeated mucosal inflammation from cycles of DSS can induce colitis and colitis-associated colorectal cancer through mechanisms such as genetic mutation, changes in crypt cell metabolism, changes in intestinal bile acid circulation and alterations in bacterial flora.[2]

DSS is a colonic non-genotoxic carcinogen, which causes injury to the epithelial barrier that can affect protein folding in the endoplasmic reticulum (ER) and cause ER stress. It is also a large and negatively charged molecule, which can not easily cross membranes and was found in 6 to 7 week old Female BALB/c Cr Slc mice to be distributed in the liver, the mesenteric lymph node, and the large intestine 1 day after the start of administration.[22] In response to the damage, lymphocytes are activated and there is an initial Th1 response which includes a subset of helper-inducer T-lymphocytes that synthesize and secrete interleukin-2 (IL-2), gamma-interferon, and IL-12.[23] After chronic inflammation, there is a combination Th1 and Th2 (subset of helper-inducer T-lymphocytes which synthesize and secrete the interleukins IL-4, IL-5, IL-6, and IL-10) response.[23, 24] Large amounts of secreted tumor necrosis factor alpha (TNF-α) and IL-6

cause most of the tissue damage. DSS induces inflammatory infiltration of the mucosa propria, ulceration, and bloody diarrhea which are characteristic of human colitis.[10]

AOM is a colonic genotoxic carcinogen, which induces methylation damage including many substrates for *Aag* such as 3MeA and also O^6MeG, a substrate for *Mgmt*. It activates the intrinsic tyrosine kinase of the epidermal growth factor (EGF) receptor while stimulating the synthesis of transforming growth factor alpha (TGF-α).[25] Tumors are induced in the distal colon. It had been shown previously that initiation with a low does of AOM exerts tumor promoting activity.[2] AOM requires metabolic activation of Cytochrome P450 2E1 (CYP2E1) to exert carcinogenic action.[2]

The reasons for choosing this model are based on results from many publications, which verify the simplicity of induction, immediate inflammation, and high reproducibility of the model. Also, the ability of the model to induce tumor formation was attractive as the Samson Lab studies DNA damage and repair and progression to cancer. Table 1 gives a summary of results from a few of the many publications using variations of the DSS model.

Publication	Treatment	Mouse Strain	Results
[10]	9 cycles of 3% DSS (7 days DSS, 14 days water), sac'd on day 189	8 week old CBA/J female mice (n=25)	3 mice 2 lesions, 9 mice 1 lesion: 9 low-grade dysplasias, 4 high-grade dysplasias, 2 invasive carcinomas
[2]	10 mg/kg AOM, 7 days 2% DSS, sac'd week 20 (140 days)	6 week old male Crj: CD-1 (ICR) (n=8)	3 adenomas (0.2 multiplicity), 8 adenocarcinomas (5.6 multiplicity)
[14]	2 cycles of 4% DSS (7 days DSS, 14 days water), sac'd 126 days	8 week old C57BL/6 x CBA (n=15)	2/15 mice, 1 low grade neoplasia, 2 invasive neoplasias
[1]	10 mg/kg AOM, 7 days 2% DSS, sac'd 2, 3, 4, 5, 6, 9, 12, 14 weeks	6 week old male ICR mice	Adenocarcinomas development by week 4 6, 9, 12, and 14 week groups all had adenocarcinomas with 100% incidence and varying degrees of invasion
[26]	10 mg/kg AOM, 2%, 1%, 0.5%, 0.25%, 0.1% DSS for 1 week, sac'd week 14		AOM w/ 2% DSS treatment gave 100% incidence of adenocarcinomas with severe inflammation and nitrosation stress
[8]	12.5 mg/kg AOM, 2 cycles with 5 days of 2.5% DSS, 1 cycle of 2% DSS	6-8 week old $Ikk\beta^{F/\Delta}$ and $Ikk\beta^{F/F}$ mice	~ 20 tumors per mouse

Table 1. Previous results with DSS and AOM/DSS mouse models.

Genetic background is important to the response, so all treated and control animals used in this experiment are C57BL/6 background. C57BL/6 mice seem to be fairly sensitive to AOM plus DSS treatment when compared with Balb/c, C3H/HeN, and DBA/2N mouse strains.[27] Also animals 6-8 weeks old had already been used in the majority of similar studies, and so would make a more relevant comparison to previous experiments. The procedure followed in the following experiments was derived from the paper by Greten et al. (reference number [8]) because of the high tumor incidence (see Table 1). At

the start of the experiment, it was not known if the *Aag*$^{-/-}$ background of the mice would protect against or enhance the effects of chronic inflammation, so a high tumor incidence would leave room for either phenotype.

1.5 Specific aims

- To determine the consequences of chronic inflammation due to inflammatory bowel disease, modulated by the absence of *Aag* substrate repair
- To determine pathological differences given chronic inflammation and a tumor initiation event, modulated by the absence of Aag substrate repair
- To determine if differences in pathology are due to accumulation of DNA lesions or inherent differences in inflammatory processes in 3-methyladenine-DNA-glycosylase deficient (*Aag*$^{-/-}$) mice

Chapter 2: Experimental Methods

2.1 Mouse Information

All animals were C57BL/6 background and were 6-8 weeks old at the start of the experiments. Animals were housed in the MIT mouse facilities in building 68 south room 0004. Table 2 shows a list of the number and type of mice used for each treatment group.

Treatment	Genotype	Total Number of Animals	Number of Males	Number of Females
AOM + DSS	Wild Type	15	9	6
AOM + DSS	*Aag*$^{-/-}$	34	11	23
AOM + DSS	*Mgmt*$^{-/-}$	6	1	5
DSS	Wild Type	10	10	0
DSS	*Aag*$^{-/-}$	10	5	5
DSS	*Mgmt*$^{-/-}$	5	5	0
AOM	Wild Type	5	5	0
AOM	*Aag*$^{-/-}$	6	0	6
AOM	*Mgmt*$^{-/-}$	6	3	3
Untreated	Wild Type	5	4	1
Untreated	*Aag*$^{-/-}$	8	5	3
Untreated	*Mgmt*$^{-/-}$	8	3	5

Table 2. Treatments, mouse type, and number of animals used.

2.2 Treatments

To determine the consequences of chronic inflammation due to IBD, modulated by the absence of *Aag* substrate repair, wild type and $Aag^{-/-}$ mice were treated with cycles of DSS to induce chronic inflammation. To determine pathological differences given chronic inflammation and a tumor initiation event, modulated by the absence of *Aag* substrate repair, wild type and $Aag^{-/-}$ mice were treated with AOM as a tumor initiator plus cycles of DSS to induce chronic inflammation. Mice were also treated with AOM alone to determine if which effects if any were due to the initiator.

2.2.1 DSS

Figure 7 shows the treatment scheme for mice given only DSS. The experiment started on day 0 and mice were sacrificed on day 100. Each cycle of DSS was 2.5% Dextran Sulfate Sodium (MP Biomedicals) in distilled water except the last cycle which was 2% DSS. Cycle 1 was days 5 to 9, cycle 2 was days 26 to 30, cycle 3 was days 47 to 51, cycle 4 was days 68 to 72, and cycle 5 was days 89 to 92. Mice were weighed at the beginning of the experiment, at the beginning and end of each cycle, and at the end of the experiment.

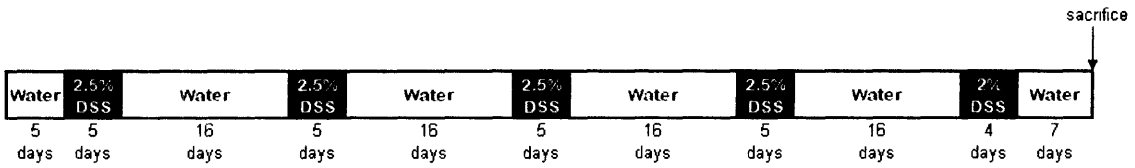

Figure 7. Mice were treated with DSS. White blocks represent 16 days of normal water except the last which is 7 days. Black blocks represent 5 days of 2.5% DSS in water except for the last, which is 4 days of 2% DSS.

2.2.2 AOM

Figure 8 shows the treatment scheme for mice given only one injection of 12.5 mg/kg AOM. The experiment started on day 0 and mice were sacrificed on day 100. The mice drank normal water for the entire experiment and were not given any DSS. The mice were still weighed at the beginning of the experiment, at the beginning and end of each cycle, and at the end of the experiment.

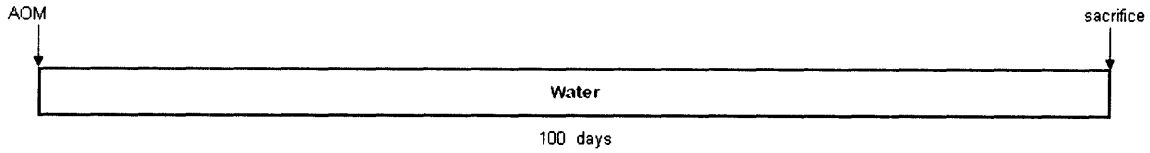

Figure 8. Mice were treated with AOM. White blocks represent normal water.

2.2.3 AOM and DSS

Figure 9 shows the treatment scheme for mice given AOM and DSS. The experiment started on day 0 and mice were sacrificed on day 100. A single does of 12.5 mg/kg AOM

was given on day 0. Each cycle of DSS was 2.5% Dextran Sulfate Sodium (MP Biomedicals) in distilled water except the last cycle which was 2% DSS. Cycle 1 was days 5 to 9, cycle 2 was days 26 to 30, cycle 3 was days 47 to 51, cycle 4 was days 68 to 72, and cycle 5 was days 89 to 92. Mice were weighed at the beginning of the experiment, at the beginning and end of each cycle, and at the end of the experiment.

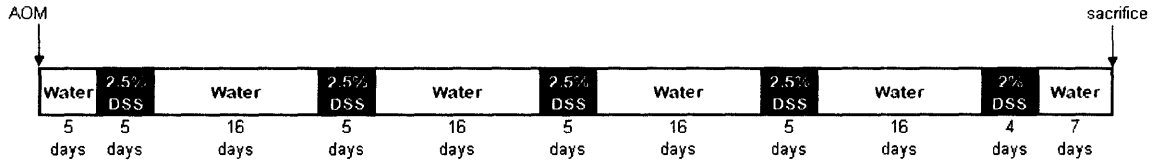

Figure 9. Mice were treated with AOM and DSS. White blocks represent 16 days of normal water except the last which is 7 days. Black blocks represent 5 days of 2.5% DSS in water except for the last, which is 4 days of 2% DSS.

2.3 Sacrifice Procedure

Animals were injected with 100 mg/kg BrdU 2.5 hours before sacrifice. Animals were sacrificed by CO_2 inhalation for at least 1 minute beyond apparent death as dictated by the Committee on Animal Care. Intestines and spleens were removed and in some cases lymph nodes or other abnormal tissues. The intestine was cut at the anus and cecum, was washed out with phosphate buffered saline (PBS), and was cut open and measured. Photographs were taken and polyps were counted using a stereomicroscope and lifting the edges of each polyp with tweezers to distinguish between individual polyps. Intestines were cut in half longitudinally. Half was fixed in formalin for 4 hours and

transfer to ethanol, and half was frozen for extracting protein or DNA. Spleens were weighed and cut in half for fixing and freezing.

2.4 Tissue Processing

Tissues were taken to the Center for Cancer Research histology lab to be paraffin embedded and cut and stained on slides by Alicia Caron. Hematoxylin and Eosin slides were then taken to Dr. Arlin Rogers for scoring. Scores were given for inflammation, epithelial defects, crypt atrophy, dysplasia/neoplasia, and area affected by dysplasia and neoplasia. Scoring criteria as written by Dr. Rogers is shown in the Pathology Results section.

2.5 Statistical Analysis

GraphPad Prism software was used for all statistical analyses. The Mann-Whitney test was used to compare quantitative results as well as scoring data. The Mann-Whitney test is a nonparametric test used to compare two unpaired groups. Fisher's exact test was used to compare tumor incidence. Fisher's exact test is a statistical test used to determine if two categorical variables exhibit nonrandom associations.

Chapter 3: Experimental Results

3.1 *Aag*$^{-/-}$ mice treated with DSS exhibit a phenotype

Previously, there have been no published phenotypes for *Aag*$^{-/-}$ mice treated with damaging agents. A phenotype is important because it can allow a model to be used for determining the role of a particular gene or the effect of a treatment for disease. There was rationale in thinking that *Aag*$^{-/-}$ mice might show a phenotype when treated chronically with DSS since *Aag* plays a role in the repair of DNA damage induced by chronic inflammation.

Wild type and *Aag*$^{-/-}$ mice were treated with DSS to determine the consequences of chronic inflammation due to IBD, modulated by the absence of *Aag* substrate repair. Signs of increased disease, such as spleen weight, body weight, and colon length, were measured in this experiment. Since about 5% of patients with colitis go on to develop colon cancer, mouse intestines were also visually inspected for polyp formation, and any polyps were counted using a stereomicroscope.

3.1.1 Polyp Formation

Polyp multiplicity and incidence are important measures of disease progression. Multiplicity is the average number of tumors per animal and incidence is the number of animals, which developed at least one polyp out of the total number of animals. An

increase in polyp multiplicity would indicate that more of the damage induced by inflammation would lead to mutations and cell proliferation. It would be expected that *Aag*$^{-/-}$ mice would show increased polyp multiplicity and incidence under chronic inflammation conditions due to the lack of *Aag* substrate repair. This, however, was not the case for the above treatment conditions with DSS alone.

Polyps were counted by visual inspection. The results are shown in Figures 10 and 11. Figure 10 shows polyp multiplicity and Figure 11 shows polyp incidence for treatment of wild type and *Aag*$^{-/-}$ animals with DSS alone. In *Aag*$^{-/-}$ animals, the multiplicity was found to be 0.4 ± 0.7 (4 tumors in 10 animals) tumors per mouse with an incidence of 0.3 (3/10 animals with tumors). In wild type animals, the multiplicity was found to be 0.3 ± 0.5 tumors per mouse with an incidence of 0.3 (3/10 animals with tumors).

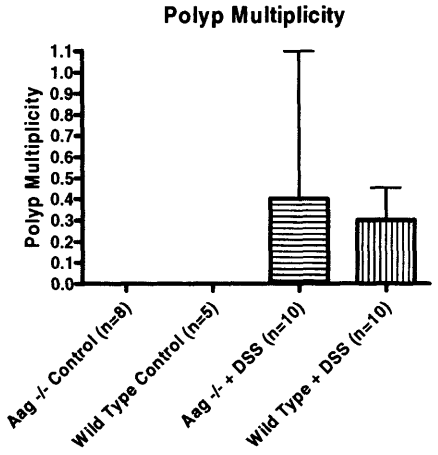

Figure 10. This graph shows polyp multiplicity, or average number of tumors per mouse. Error bars represent standard deviation. There were 10 mice treated for each genotype (n=10). There is not a significant difference in polyp multiplicity between wild type and *Aag*$^{-/-}$ animals treated with only DSS.

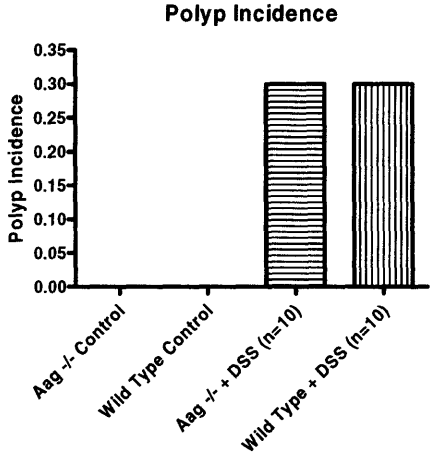

Figure 11. This graph shows polyp incidence, or number of mice out of all treated mice, which developed at least one tumor. There were 10 mice treated for each genotype (n=10). There is not a significant difference in polyp incidence between wild type and *Aag*$^{-/-}$ animals treated with only DSS.

This result indicates that for this particular treatment, there is no significant difference in the polyp formation between wild type and *Aag*$^{-/-}$ animals. The fact that both genotypes developed polyps confirms that DSS acts as both an initiator and a promoter. Figure 12 shows representative photos of DSS treated intestines and untreated intestines for comparison. *Aag*$^{-/-}$ intestines appeared bumpier than wild type intestines. Although there were not significant differences in polyp multiplicity or incidence between wild type and *Aag*$^{-/-}$ mice, there was found to be a significant difference in epithelial defects which is shown in Figure 29 in the Pathology Results section. Significant differences were also seen in other indicators of increased disease discussed below.

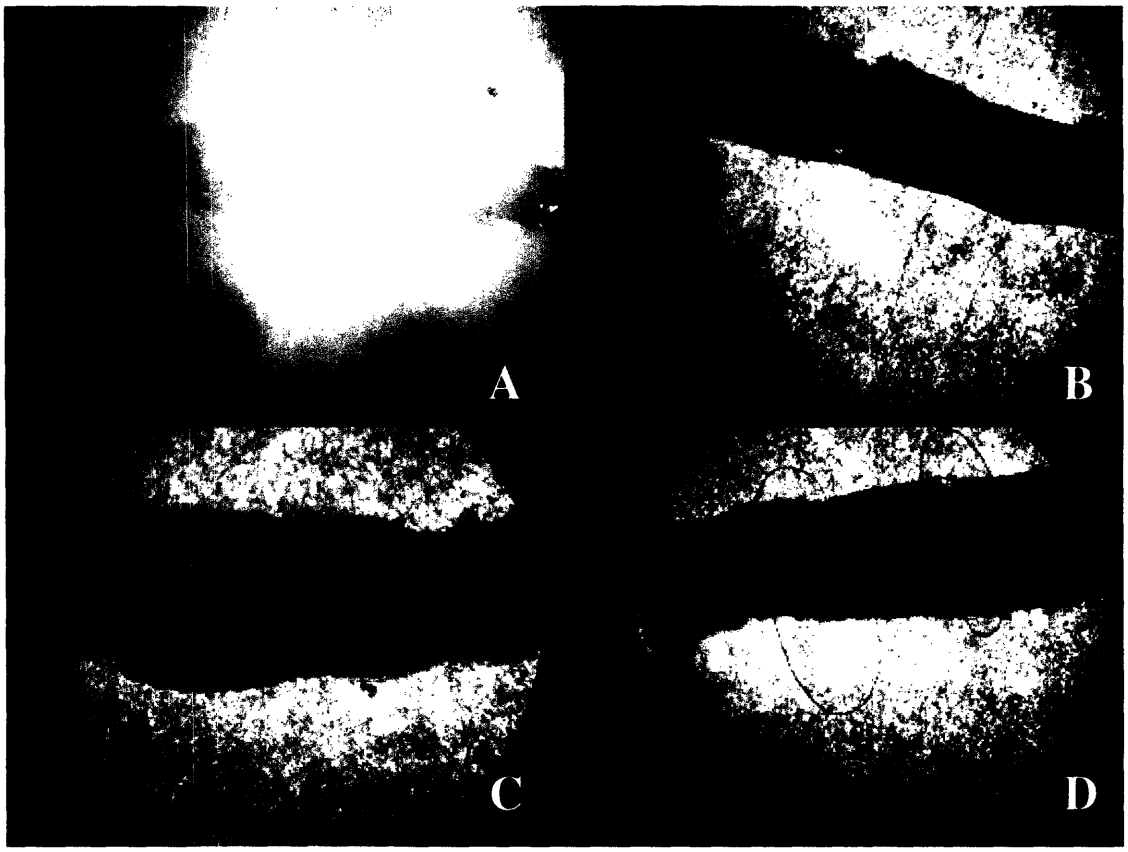

Figure 12. A: Wild type untreated intestine. B: *Aag*$^{-/-}$ untreated intestine. C: Wild type intestine from DSS treated animal. Region of hyperplasia and possible pre-polyp can be seen on the left. D: *Aag*$^{-/-}$ intestine from DSS treated animal. Inflammation and hyperplasia cause the intestine to look rough.

3.1.2 Colon Length

Polyp formation is not the only sign of increased IBD in mice. Another indicator is colon length, which is known to decrease with increased disease due to healing ulcers and fistulas. Cycles of DSS induce chronic inflammation which leads to lipid peroxidation and the production of RONS. On top of DNA damage, RONS damage proteins and lipids and DSS itself affects protein folding causing ER stress. Unrepaired DNA damage

could leads to even more cell death and apoptosis, requiring more healing, and consequently a decrease in colon length.

It was found that *Aag*$^{-/-}$ mice treated with DSS show a significantly greater change in length than wild type mice treated with DSS. Figures 13 and 14 show these results. Figure 13 shows a graph of colon length and Figure 14 shows a graph of change in colon length from control animals treated with DSS alone. In *Aag*$^{-/-}$ animals, the average colon length of DSS treated animals was found to be 5.7 ± 0.7 cm with a change in colon length of -2.7 ± 0.7 cm. In *Aag*$^{-/-}$ untreated animals, the average colon length was found to be 8.5 ± 0.6 cm. In wild type animals, the average colon length of DSS treated animals was found to be 6.7 ± 0.9 cm with a change in colon length of -0.4 ± 0.6 cm. In wild type untreated animals, the average colon length was found to be 7.3 ± 0.6 cm.

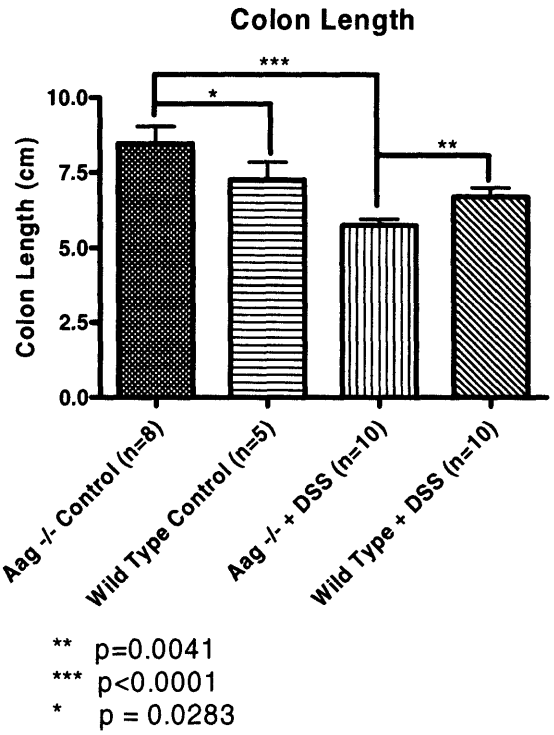

Figure 13. This graph shows colon length data. Since *Aag*$^{-/-}$ control and wild type control lengths were found to be significantly different, the change in colon length from control to treated is important to look at.

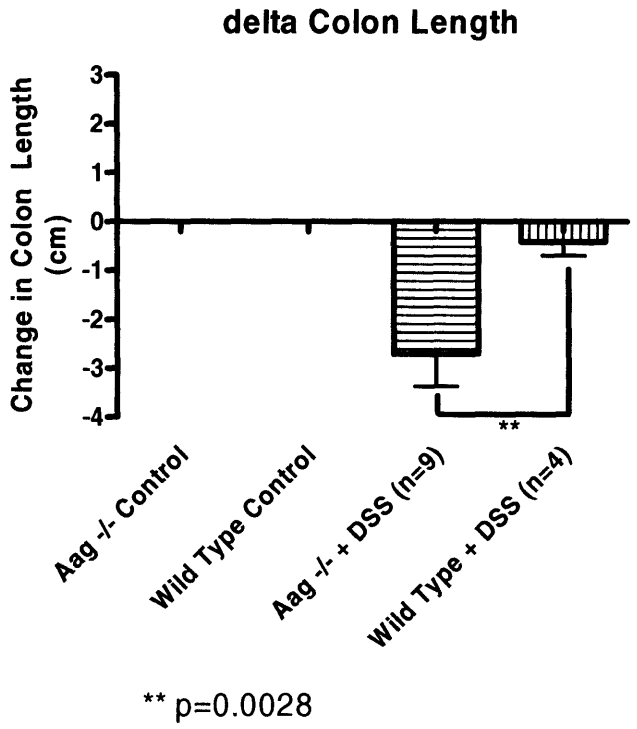

Figure 14. This graph shows change in colon length from the control length. Since *Aag*$^{-/-}$ control and wild type control lengths were found to be significantly different, the change in colon length from control to treated is important to look at. This change is significantly different between wild type and *Aag*$^{-/-}$ animals treated only with DSS (p=0.0028).

This result indicates that for this particular treatment, there is a significant difference in change in colon length between wild type and *Aag*$^{-/-}$ animals with a p-value of 0.0028. Both animal types showed a decrease in colon length, which as mentioned above, is an indication of healing ulcers and fistulas. Even though there was no significant difference in polyp formation between the two genotypes, there is indication of more severe disease in the *Aag*$^{-/-}$ animals. This is the first phenotype to be described for *Aag*$^{-/-}$ animals treated with a damaging agent.

3.1.3 Spleen and Body Weight

In addition to colon length, another indicator of increased disease in mice is spleen weight. During IBD, there is blood loss through stools that reduces the number of blood cells and platelets in the blood stream. The spleen is involved in the production and maintenance of red blood cells and enlarges due to increased red blood cell production and increased trapping of red blood cells and platelets. It could be expected that *Aag*$^{-/-}$ animals would have more ulceration and blood loss and thus increased spleen weight compared to wild type animals when treated with DSS. This was in fact shown for these experimental conditions. The spleen weight results are shown in Figure 15 as a percent of final body weight. In addition, blood loss and disease lead to decreased appetite and body weight. As expected, *Aag*$^{-/-}$ mice showed significantly lower body weights after day 26 of the experiment. Figure 16 shows body weight results as percent change in body weight from the animals' original body weight.

As shown in Figure 15, the average spleen weight of *Aag*$^{-/-}$ mice treated with DSS was found to be 0.55 ± 0.19 % of final body weight. *Aag*$^{-/-}$ untreated animals have an average spleen weight of 0.25 ± 0.01 % of final body weight. In wild type animals, the average spleen weight of DSS treated animals was found to be 0.28 ± 0.14 % of final body weight. In wild type untreated animals, the average spleen weight was found to be 0.26 ± 0.03 % of final body weight. As shown in Figure 16, percent change in body weight was similar for the first 25 days of treatment and became significantly different on day 26.

This difference increased for the remainder of the experiment. P-values can be seen in Table 3.

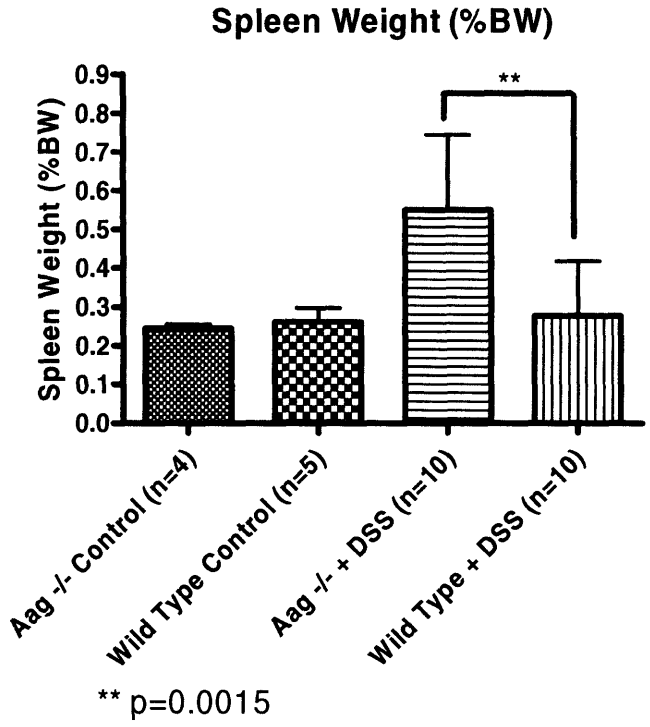

Figure 15. This graph shows spleen weight as a percentage of final body weight. Spleen weights of *Aag*$^{-/-}$ animals are significantly greater than wild type animals when treated with DSS (p=0.0015).

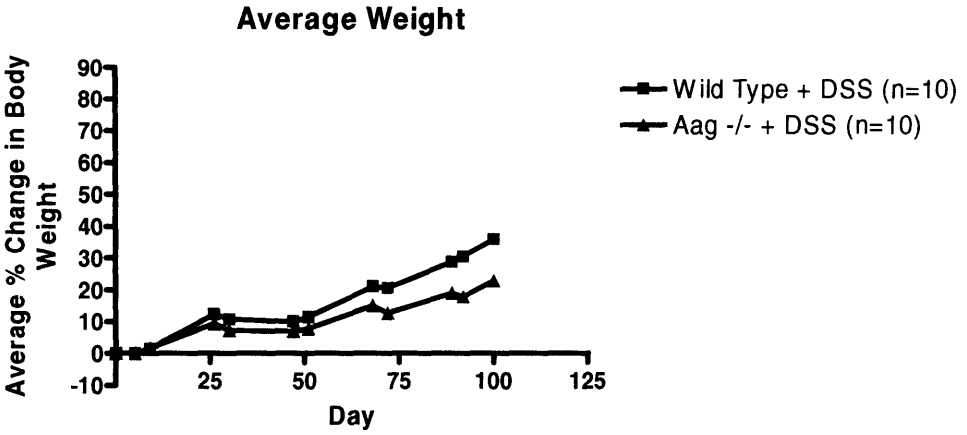

Figure 16. This graph shows the average percent change in body weight vs. days of treatment. Change in body weight of wild type animals was significantly greater than *Aag*$^{-/-}$ animals after day 26 (See Table 3).

* p=0.0115	Day 26
* p=0.0115	Day 30
* p=0.0433	Day 47
* p=0.0433	Day 51
** p=0.0029	Day 68
*** p=0.0007	Day 72
*** p=0.0002	Day 89
*** p<0.0001	Day 92
*** p<0.0001	Day 100

Table 3. P-values for significance of differences in percent change in body weight between wild type and *Aag*$^{-/-}$ animals treated with DSS alone.

The results of this experiment suggest that there is a difference in the wild type and *Aag*$^{-/-}$ animals' response to chronic inflammation. In *Aag*$^{-/-}$ animals, spleen weight was significantly increased and colon length was significantly decreased. These are two indications of increased disease in UC. As these results are the first phenotype to be seen in *Aag*$^{-/-}$ mice, they are extremely encouraging and motivate further study of the role of *Aag* in inflammation and cancer. In order to determine if *Aag*$^{-/-}$ animals would have an increased tumor response compared to wild type given initial damage, animals were treated with a tumor initiation agent prior to inducing chronic inflammation.

3.2 *Aag*$^{-/-}$ mice treated with AOM plus DSS exhibit a dramatic phenotype

Given the results of the previous section, it is clear that *Aag* is contributing to prevention of the harmful effects of chronic inflammation. It was formerly unclear whether or not the deletion of *Aag* would lead to sensitivity or resistance in the whole animal model since previous manipulation of this repair in cultured cell lines has led to surprising results. Although it is interesting to see a phenotype from DSS treatment alone, the initial aim of this project was in studying inflammation and cancer, as many IBD patients go on to develop colorectal cancer. This section discusses the results of treating mice with a tumor initiator prior to induction of chronic inflammation.

Wild type and *Aag*$^{-/-}$ mice were treated with AOM plus DSS to determine the consequences of a tumor initiation event along with chronic inflammation due to IBD, modulated by the absence of *Aag* substrate repair. Mice were also treated with AOM

alone to determine any background effects of the tumor initiator. Signs of increased disease in mice include increased spleen weight, decrease in body weight, and decreased colon length, which were measured in this experiment. Mouse intestines were also visually inspected for polyp formation and any polyps were counted using a stereomicroscope.

3.2.1 Polyp Number

As previously stated, polyp multiplicity and incidence are important measures of disease progression. Although no significant differences in polyps were seen with DSS treatment alone, there were indicators of increased disease. It would therefore be expected that *Aag*$^{-/-}$ mice would show some difference in polyp multiplicity and incidence under chronic inflammation conditions due to the lack of *Aag* substrate repair. With the addition of a tumor initiator, *Aag*$^{-/-}$ mice indeed show a significant increase in tumor multiplicity. These results are shown in Figures 17 and 18.

Figure 17 shows polyp multiplicity and Figure 18 shows polyp incidence for treatment of wild type and *Aag*$^{-/-}$ animals with AOM and DSS. In *Aag*$^{-/-}$ animals, the multiplicity was found to be 21.6 ± 8.2 tumors per mouse with an incidence of 1.0 (all mice developed polyps). In wild type animals, the multiplicity was found to be 7.7 ± 6.7 tumors per mouse with an incidence of 1.0 (all mice developed polyps).

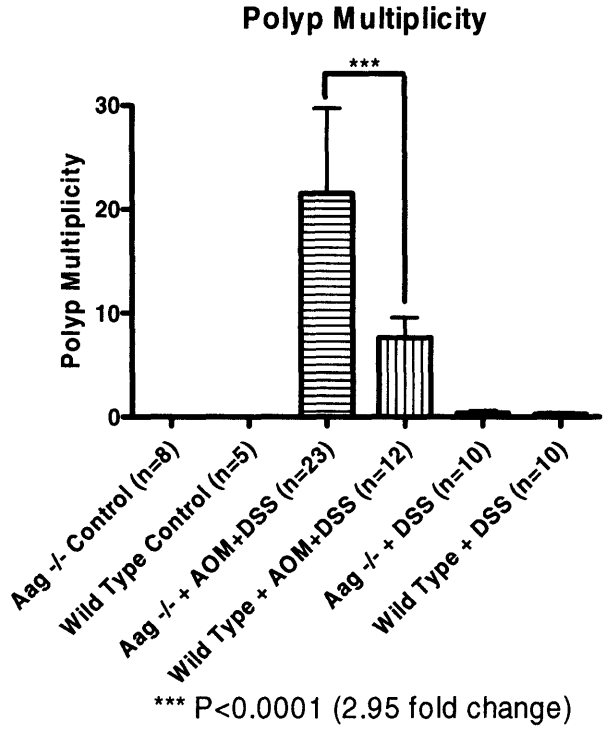

Figure 17. This graph shows polyp multiplicity, or average number of tumors per mouse. Error bars represent standard deviation. There were 23 *Aag*$^{-/-}$ mice and 12 wild type mice treated with AOM and DSS and counted for tumors. There is a significant difference in polyp multiplicity (2.95 fold, p<0.0001). DSS data is from Figure 10.

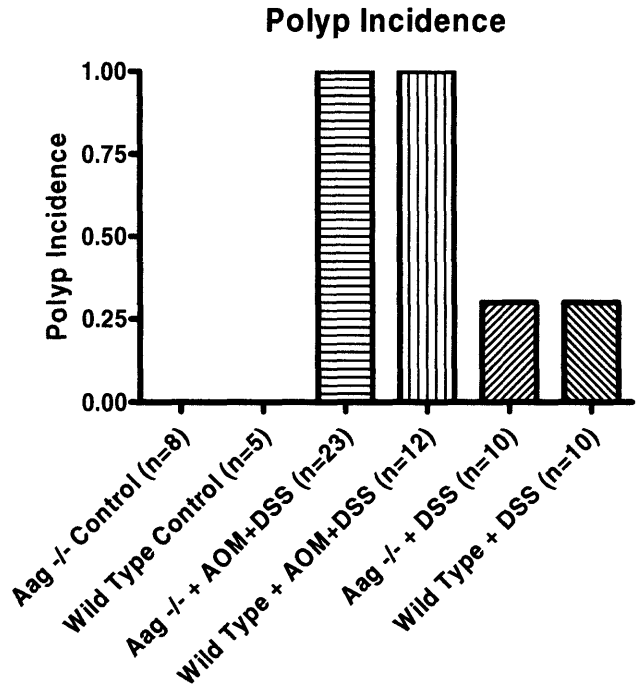

Figure 18. This graph shows polyp incidence, or number of mice out of all treated mice, which developed at least one tumor. Error bars represent standard deviation. There were 23 *Aag*$^{-/-}$ mice and 12 wild type mice treated with AOM and DSS and counted for tumors. There is not a significant difference in polyp incidence between wild type and *Aag*$^{-/-}$ animals. DSS data is from Figure 11.

This result indicates that for treatment with AOM and DSS, there is a 2.95 fold difference ($p>0.0001$) in the polyp formation between wild type and *Aag*$^{-/-}$ animals. This means that when given a tumor initiator, *Aag*$^{-/-}$ mice are much more likely to develop a polyp than wild type mice. When treated with AOM alone, neither wild type nor *Aag*$^{-/-}$ animals developed polyps. This means that a single initiation is not enough to cause tumor formation, and chronic inflammation is necessary to promote tumor development. Figure 19 shows representative photos of intestines from AOM treated mice and AOM plus DSS

treated mice. Intestines from mice treated with AOM alone look similar to the untreated photos shown above. Polyps can be seen in intestines from mice treated with AOM and DSS.

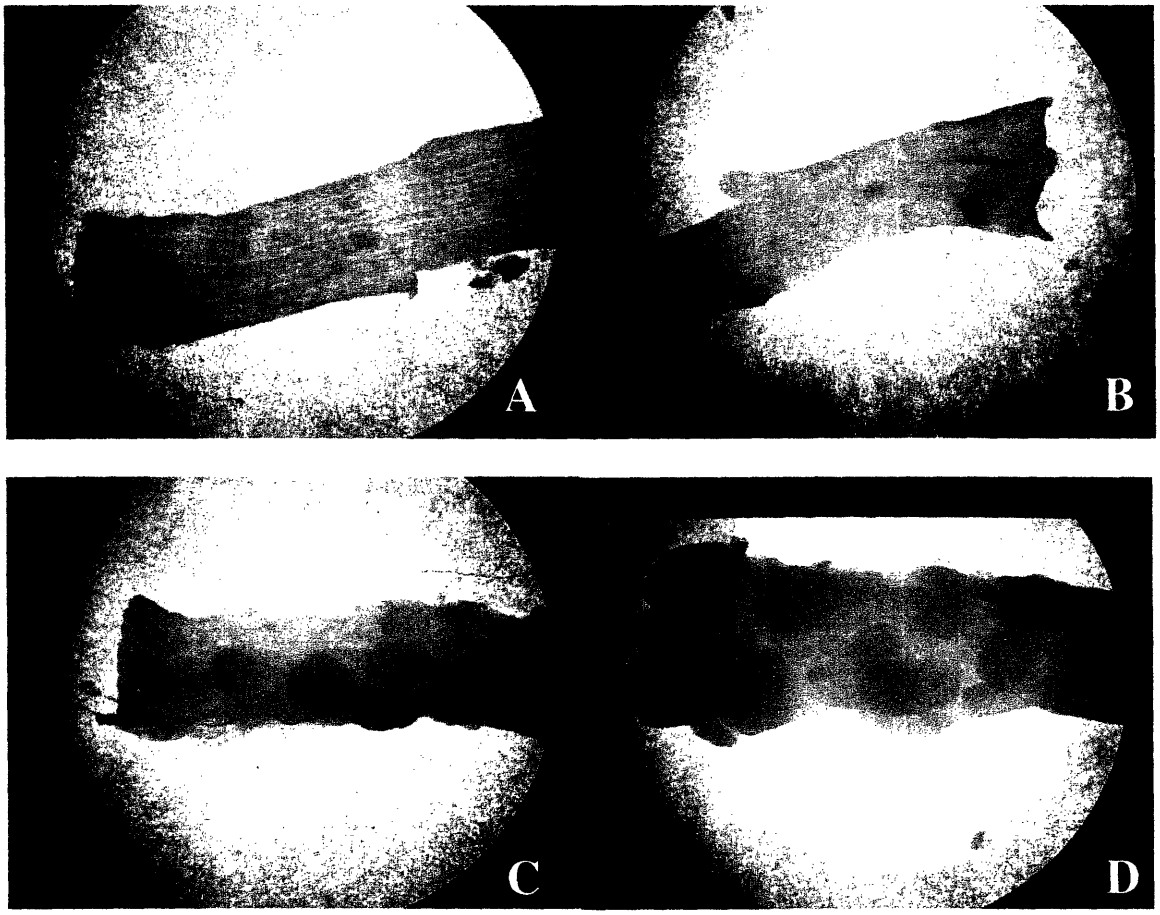

Figure 19. A: Wild type intestine from AOM treated animal. B: *Aag*$^{-/-}$ intestine from AOM treated animal. C: Wild type intestine from AOM and DSS treated animal. This particular animal had 7 polyps which is about average. D: *Aag*$^{-/-}$ intestine from AOM and DSS treated animal. This particular mouse had 29 polyps which is about 7 more than average.

This result is very exciting because of the dramatic phenotype seen in *Aag*$^{-/-}$ mice and because polyps are generally a precursor to cancer and are easy to measure in vivo as an indicator of disease. This also indicates the need to carry out a longer experiment to determine whether or not the polyps eventually develop into cancer. As before, other indicators of IBD were also measured.

3.2.2 Colon Length

With the addition of a tumor initiator, it would be expected that there could be even greater changes in colon length than with DSS alone, since AOM also causes some damage to DNA. Results show however, that with AOM alone, *Aag*$^{-/-}$ colons only decrease slightly, while wild type colons increase slightly, and with AOM plus DSS treatment, changes in colon length are almost the same as with DSS alone. Changes in colon lengths are significantly different between *Aag*$^{-/-}$ and wild type mice treated with AOM alone or AOM plus DSS, however colon length results from AOM alone and DSS alone are neither additive nor synergistic. These results are shown in Figures 20 and 21.

Figure 20 shows a graph of colon length and Figure 21 shows a graph of change in colon length from control animals treated with AOM alone and AOM plus DSS respectively. In *Aag*$^{-/-}$ animals, the average colon length of AOM treated animals was found to be 7.5 ± 1.3 cm with a change in colon length of -1.0 ± 1.3 cm. In *Aag*$^{-/-}$ animals, the average colon length of AOM plus DSS treated animals was found to be 6.0 ± 0.6 cm with a change in colon length of -2.5 ± 0.6 cm. In *Aag*$^{-/-}$ untreated animals, the average colon

length was found to be 8.5 ± 0.6 cm. In wild type animals, the average colon length of AOM treated animals was found to be 8.4 ± 0.8 cm with a change in colon length of 1.1 ± 0.8 cm. In wild type animals, the average colon length of AOM plus DSS treated animals was found to be 6.5 ± 0.8 cm with a change in colon length of -0.8 ± 0.8 cm. In wild type untreated animals, the average colon length was found to be 7.3 ± 0.6 cm.

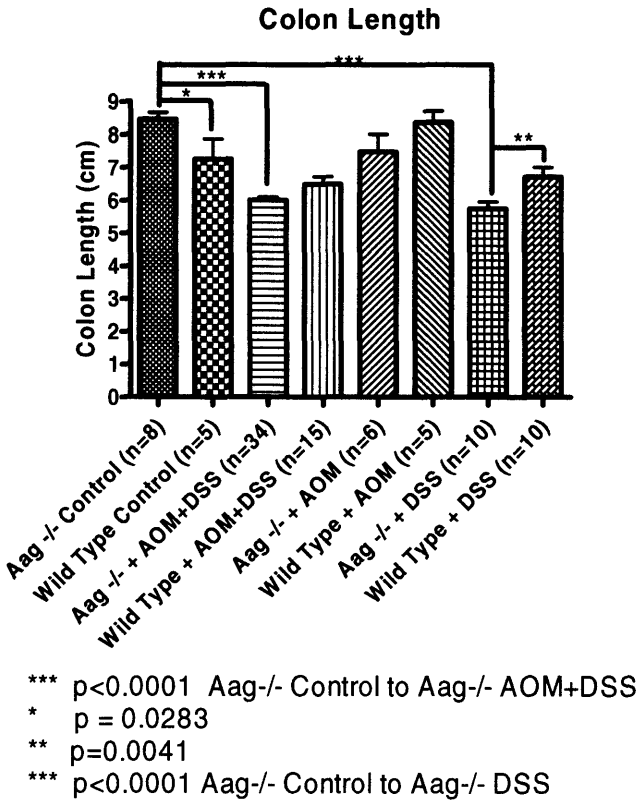

Figure 20. This graph shows colon length for AOM only and AOM plus DSS treated animals. Since *Aag*$^{-/-}$ control and wild type control lengths were found to be significantly different, the change in colon length from control to treated is important to look at. DSS data is from Figure 13.

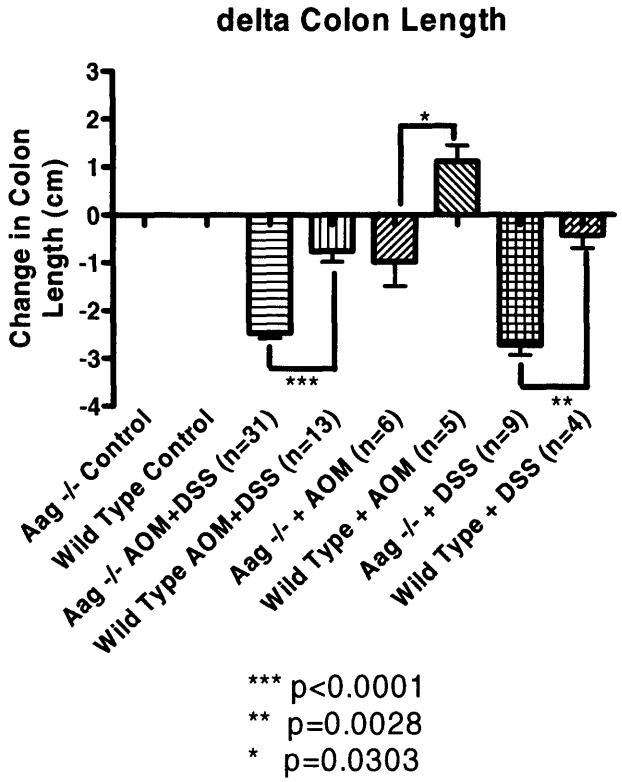

Figure 21. This graph shows change in colon length. Since *Aag*$^{-/-}$ control and wild type control lengths were found to be significantly different, the change in colon length from control to treated is important to look at. This change is significantly different between wild type and *Aag*$^{-/-}$ animals treated with AOM and DSS (p=0.0028), AOM alone (p=0.0303), and DSS alone (p=0.0028). DSS data is from Figure 14.

This result indicates that for treatment with AOM, there is a significant difference in change in colon length between wild type and *Aag*$^{-/-}$ animals with a p-value of 0.0303. *Aag*$^{-/-}$ animals showed a small decrease in colon length, whereas wild type animals showed a small increase in colon length. When treated with AOM plus DSS, both genotypes show a decrease in colon length and the change in length from controls was

significantly different between the two with a p-value of less than 0.0001. The AOM seems to have a modest effect on the *Aag*$^{-/-}$ animals, but when treated with DSS, the differences between wild type and *Aag*$^{-/-}$ animals are dramatically increased. Both animal types show a similar change in colon length to those treated with DSS alone.

3.2.3 Spleen and Body Weight

As mentioned in the previous section, the spleen is involved in the production and maintenance of red blood cells and enlarges due to increased red blood cell production and increased trapping of red blood cells and platelets. It would be expected that *Aag*$^{-/-}$ animals treated with AOM plus DSS could have more ulceration and blood loss due to a larger amount of damage and thus increased spleen weight compared to wild type animals. This was in fact shown for these experimental conditions. The spleen weight results are shown in Figure 22 as a percent of final body weight. In addition, it would be expected that the tumor initiator would lead to increased sickness, which would cause a decrease in body weight. *Aag*$^{-/-}$ mice treated with AOM and DSS showed significantly lower body weights on days 72, 89, and 92 of the experiment, however did not appear to show much difference than when treated with DSS alone. In contrast, wild type animals treated with AOM plus DSS show a decrease in body weight compared to treatment with DSS alone. *Aag*$^{-/-}$ mice treated chronically with DSS get very sick and lose weight, so it is possible that the *Aag*$^{-/-}$ animals are at a lower weight limit and won't lose any extra weight with the addition of AOM. Figure 23 shows body weight results as percent change in body weight from the animals' original body weight.

In *Aag*$^{-/-}$ animals, the average spleen weight of AOM treated animals was found to be 0.42 ± 0.05 % of final body weight. In *Aag*$^{-/-}$ animals, the average spleen weight of AOM plus DSS treated animals was found to be 0.81 ± 0.49 % of final body weight. In *Aag*$^{-/-}$ untreated animals, the average spleen weight was found to be 0.25 ± 0.01 % of final body weight. In wild type animals, the average spleen weight of AOM treated animals was found to be 0.27 ± 0.04 % of final body weight. In wild type animals, the average spleen weight of AOM plus DSS treated animals was found to be 0.60 ± 0.20 % of final body weight. In wild type untreated animals, the average spleen weight was found to be 0.26 ± 0.03 % of final body weight. Percent change in body weight was similar for the first 8 days after AOM treatment and became significantly different on day 9. This difference increased for the remainder of the experiment. When treated with AOM plus DSS, there were significant differences in body weight between wild type and *Aag*$^{-/-}$ mice on days 72, 89, and 92. P-values can be seen in Table 4.

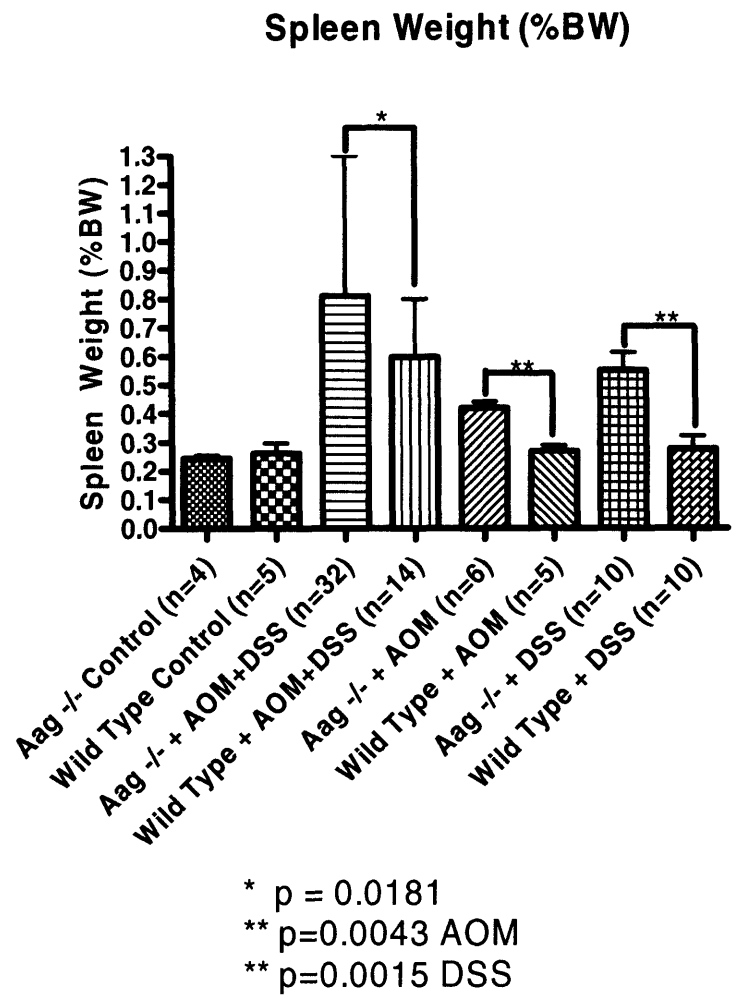

Figure 22. This graph shows spleen weight as a percentage of final body weight. Spleen weights of *Aag*$^{-/-}$ animals are significantly greater than wild type animals when treated with AOM and DSS (p=0.0181), AOM alone (p=0.0043), and DSS alone (p=0.0015). DSS data is from Figure 15.

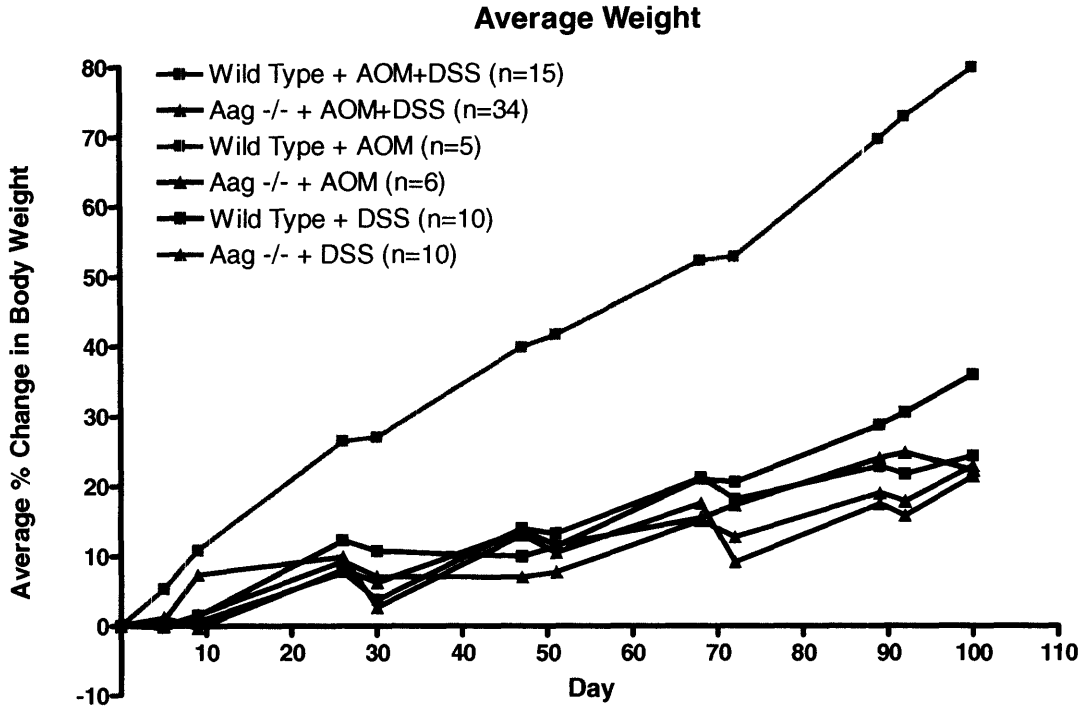

Figure 23. This graph shows the average change body weight vs. days of the experiment. Change in body weight of wild type animals was significantly greater than *Aag*$^{-/-}$ animals on days 72, 89, and 92 (See Table 4) for AOM + DSS treatment. Change in body weight of wild type animals was significantly greater than *Aag*$^{-/-}$ animals after day 9 (See Table 4) for treatment with AOM alone. Change in body weight of wild type animals was significantly greater than *Aag*$^{-/-}$ animals after day 26 (See Table 3) for treatment with DSS alone. DSS data is from figure 16.

There are significant differences in spleen weight between wild type and *Aag*$^{-/-}$ animals with AOM treatment alone (p=0.0043) as well as with AOM plus DSS treatment (p=0.0181). There are also significant differences in change in body weight after day 9 with AOM alone and on days 72, 89, and 92 for treatment with AOM plus DSS.

AOM		AOM+ DSS	
** p=0.0087	Day 9		
** p=0.0043	Day 26		
** p=0.0043	Day 30		
** p=0.0043	Day 47		
** p=0.0043	Day 51		
** p=0.0043	Day 68		
** p=0.0043	Day 72	** p=0.0019	Day 72
** p=0.0043	Day 89	* p=0.0318	Day 89
** p=0.0043	Day 92	* p=0.0466	Day 92
** p=0.0043	Day 100		

Table 4. P-values for significance of differences in percent change in body weight between wild type and *Aag*$^{-/-}$ animals treated with AOM alone and AOM plus DSS.

The results of this experiment show that there is a difference in the wild type and *Aag*$^{-/-}$ animals' response to chronic inflammation with a tumor initiation event, as significant differences were seen in polyp multiplicity, colon length, and spleen weight. In *Aag*$^{-/-}$

animals, polyp multiplicity was 2.95 times greater than wild type, spleen weight was increased and colon length was decreased. These are all indications of increased disease in UC. These results are again the first phenotype to be seen in *Aag*$^{-/-}$ mice, and are extremely encouraging because of the large difference in polyp multiplicity. The next step is to determine if this result is due to the accumulation of mutations in *Aag*$^{-/-}$ animals as would be expected, or if it could be due to some inherent difference in the inflammatory process in these mice.

3.3 Accumulation of Mutations or Inherent Difference in Inflammatory Process?

It was determined from the results of the first two aims of this project that *Aag*$^{-/-}$ animals have a significantly different phenotype than wild type animals when exposed to chronic inflammation, with or without a tumor initiation event. To determine if these differences in pathology are due to the accumulation of DNA lesions or due to some inherent difference in inflammatory processes of *Aag*$^{-/-}$ mice, a short term experiment was performed. Mice were treated with 2.5% DSS for seven days and groups were sacrificed on each of 5 days following treatment. *Aag*$^{-/-}$ mice appeared sicklier than wild type. This experiment will be continued in the lab. Slides will be analyzed by Dr. Rogers and DNA lesions will be quantified.

3.4 Antibody Results

Sections from intestine were treated with anti-BrdU and anti-Nitrotyrosine antibodies to determine if there were differences in proliferation and oxidative stress, however, staining was uneven and results are inconclusive due to the poor reproducibility. Figures 24 and 25 show results of the nitrotyrosine experiment and Figures 26 and 27 show results of the BrdU experiment.

Figure 24. Nitrotyrosine staining for an *Aag*$^{-/-}$ animal treated with AOM and DSS. Images were taken at 60x magnification.

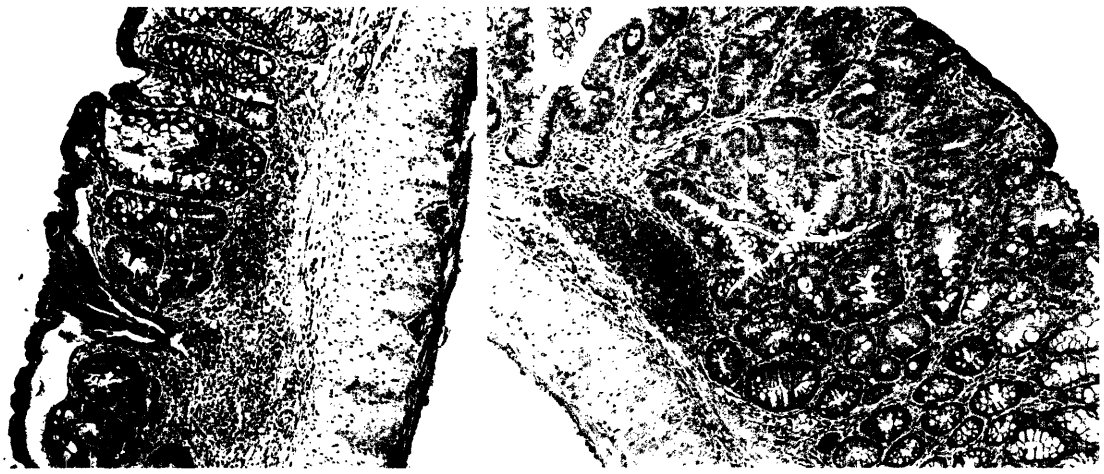

Figure 25. Nitrotyrosine staining for a wild type animal treated with AOM and DSS. Images were taken at 60x magnification.

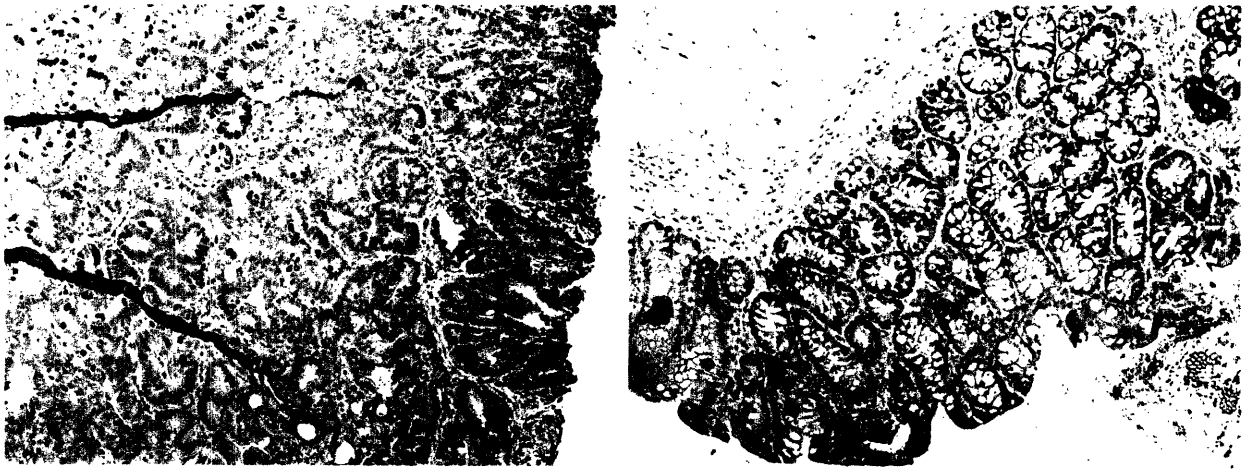

Figure 26. BrdU staining for an *Aag*$^{-/-}$ animal treated with AOM and DSS. Images were taken at 60x magnification.

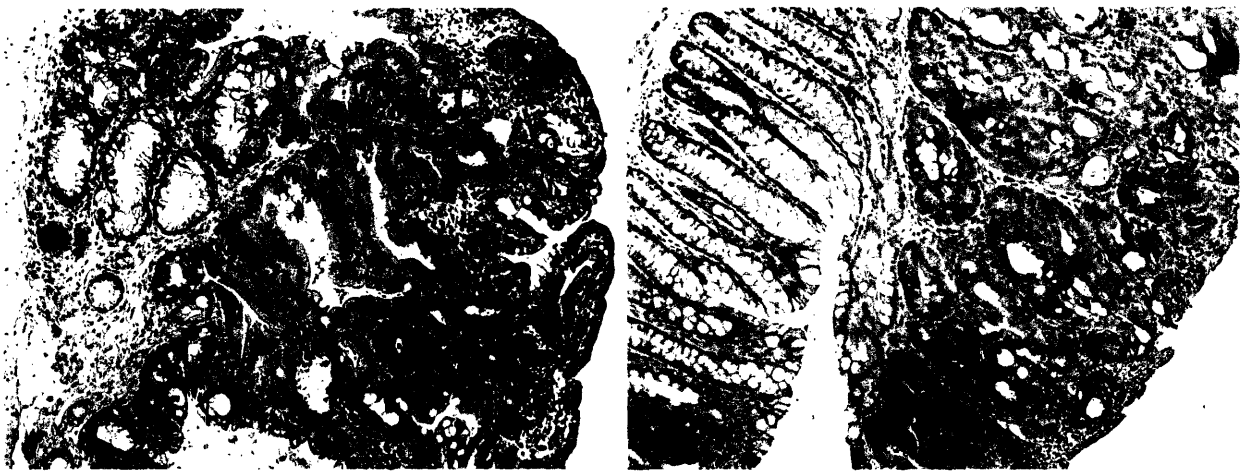

Figure 27. BrdU staining for a wild type animal treated with AOM and DSS. Images were taken at 60x magnification.

3.5 DNA Lesion Analysis

DNA was isolated from frozen sections of mouse intestine. Lesion analysis was performed on a few test samples by Koli Taghizadeh using Mass Spectrometry. The lesion analysis gave the exact opposite of what was expected as shown in Table 5. εA and εG were greatest in the wild type controls and least in *Aag*$^{-/-}$ mice treated with 5 cycles of DSS. This experiment will be redone to verify results. If lesions can be correctly quantified, all samples with all treatment schemes will be analyzed. This experiment will help test the hypothesis that the sensitivity of the *Aag*$^{-/-}$ mice when treated with DSS is due to accumulation of damaged bases.

Sample	1,N^6-εdA per 10^7 nt	1,N^2-εdG per 10^7 nt	3,N^4-εdC per 10^7 nt
Wild Type Untreated	13	4.5	Contaminated by dA (252/136), not quantifiable
Aag$^{-/-}$ Untreated	3.8	0.8	
Aag$^{-/-}$ 1 week DSS	2.6	0.4	
Aag$^{-/-}$ 5 cycles DSS	1.9	0.4	

Table 5. DNA Lesion analysis. Number 32 is a 7 week old wild type untreated mouse, number 38 is a 7 week old *Aag*$^{-/-}$ untreated mouse, number 27 is a 7 week old *Aag*$^{-/-}$ mouse treated with 1 cycle of DSS alone, and number 69 is an *Aag*$^{-/-}$ animal treated with 5 cycles of DSS alone.

3.6 Pathology Results

In addition to measuring the indicators of disease described above, Hematoxylin and Eosin stained sections of intestine on slides were scored for inflammation (Figure 28), epithelial defects (Figure 29), crypt atrophy (Figure 30), dysplasia/neoplasia (Figure 31), and area of dysplasia and neoplasia (Figure 32). Pathology analysis is important in confirming polyp formation and determining intestinal changes on the cellular level. All of the scoring was done blindly by Dr. Arlin Rogers. Scoring criteria can be seen in Table 6 and median scores for each category and treatment can be seen in Table 7.

Significant differences in score were seen for *Aag*$^{-/-}$ vs. wild type animals in epithelial defects when treated with DSS only ($p = 0.0288$), and in dysplasia/neoplasia ($p = 0.0001$) and area of dysplasia/neoplasia ($p = 0.0009$) when treated with AOM and DSS. The increase in epithelial defect score shown in Figure 29 is based on more gland dilation and surface epithelial attenuation. The increase in dysplasia/neoplasia score shown in Figure

31 is due to more crypt cells bulging toward muscularis mucosa, more piling and more cellular atypia. The increase in area of dysplasia/neoplasia score shown in Figure 32 is from less than 10% to about 10 to 25%.

These results indicate that the addition of AOM to cycles of DSS increases epithelial defects in wild type mice to the level of *Aag*$^{-/-}$ mice, and increases dysplasia/neoplasia and area of dysplasia/neoplasia in both wild type and *Aag*$^{-/-}$ mice, but more so in *Aag*$^{-/-}$ mice. There are no significant differences between groups in inflammation or crypt atrophy for any treatment, although there is inflammation seen in animals treated with DSS and AOM plus DSS. Since no differences in inflammation were seen, it is likely that the phenotype seen in *Aag*$^{-/-}$ mice is due to the lack of repair and not an inherent difference in inflammatory process from wild type mice. However, it would still be worth looking in to a time course study to confirm this and to better understand the healing process in both types of mice.

Score	Inflammation	Epithelial defects	Crypt Atrophy	Dysplasia/Neoplasia[†]	Area of Dysplasia/ Neoplasia
0	Normal	None	None	Normal	None
1	Small leukocyte aggregates in mucosa and/or submucosa	Focally dilated glands and/or attenuated surface epithelium, decreased goblet cells	<25%	Aberrant crypt foci, dysplasia characterized by epithelial cell pleomorphism, plump & attenuated forms, gland malformation with splitting, branching, and infolding	<10% surface area
2	Coalescing mucosal and/or submucosal inflammation	Focally extensive gland dilation and/or surface epithelial attenuation	~25—50%	Polypoid hyperplasia/dysplasia, moderate dysplasia characterized by pleomorphism, early cellular & nuclear atypia, piling & infolding, occasional cystic dilation, bulging towards muscularis mucosae & projection into lumen, loss of normal glandular, mucous, or goblet cells	10—25% surface area
3	Coalescing mucosal inflammation with prominent multifocal submucosal extension +/- follicle formation	Erosions (mucosal necrosis terminating above muscularis mucosae)	~50—75%	Adenomatous and/or sessile hyperplasia/dysplasia; gastrointestinal intraepithelial neoplasia (GIN) or carcinoma *in situ*, marked dysplasia confined to mucosa, features as above but greater severity, frequent & sometimes bizarre mitoses[‡]	25—50% surface area
4	Severe diffuse inflammation of mucosa, submucosa, & deeper layers	Ulceration (full-thickness mucosal necrosis extending into submucosa or deeper)	>75%	Invasive carcinoma: Submucosal invasion (differentiate from herniation) or any demonstrated invasion into blood or lymphatic vessels, regional nodes, or other metastasis	>50% surface area

[†] Dysplastic glands herniated into lymphoid follicles in an otherwise normal mucosa are not scored. Dysplasia is a normal consequence of epithelial cell herniation into GALT.
[‡] 3.5: Intramucosal carcinoma (extension of severely dysplastic regions into muscularis mucosae)

Table 6. Scoring criteria by Dr. Arlin Rogers.

MEDIAN SCORES						
		Inflammation	Epithelial Defects	Crypt Atrophy	Dysplasia /Neoplasia	Area of Dysplasia /Neoplasia
AOM/DSS	wt	2.00	1.25	0.00	1.75	1.00
	Aag -/-	2.00	1.50	0.00	2.50	2.00
	Mgmt -/-					
	wt control	0.00	0.00	0.00	0.00	0.00
DSS	wt	1.50	1.00	0.50	0.50	0.50
	Aag -/-	2.00	1.50	1.00	0.50	0.50
	Mgmt -/-	2.00	1.00	1.00	0.00	0.00
AOM	wt	0.00	0.00	0.00	0.00	0.00
	Aag -/-	0.00	0.00	0.00	0.00	0.00
	Mgmt -/-	0.00	0.00	0.00	0.00	0.00

Table 7. Median scores by category, treatment, and animal genotype. Significant differences are boxed.

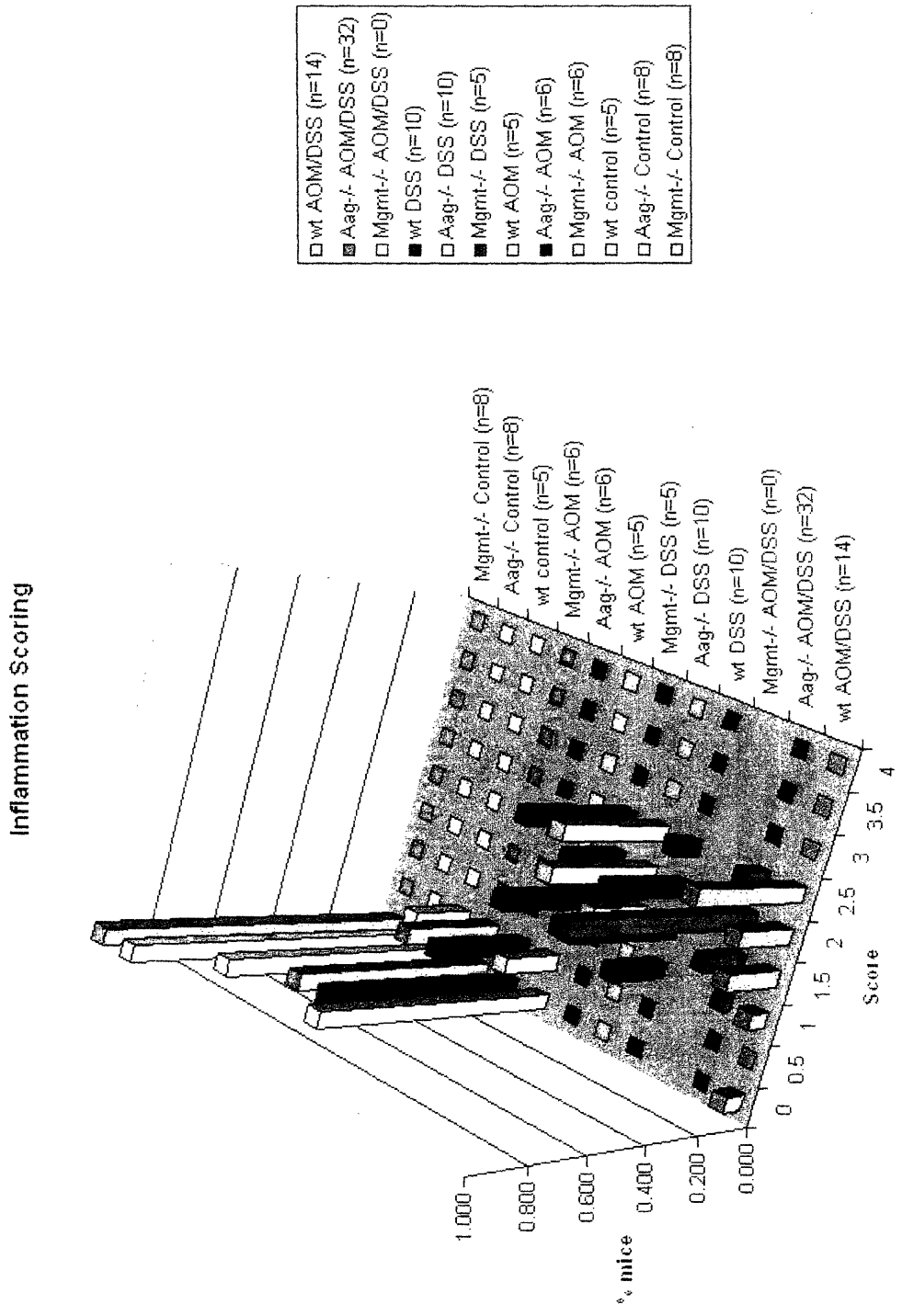

Figure 28. Inflammation scoring. There are no significant differences among treatment groups.

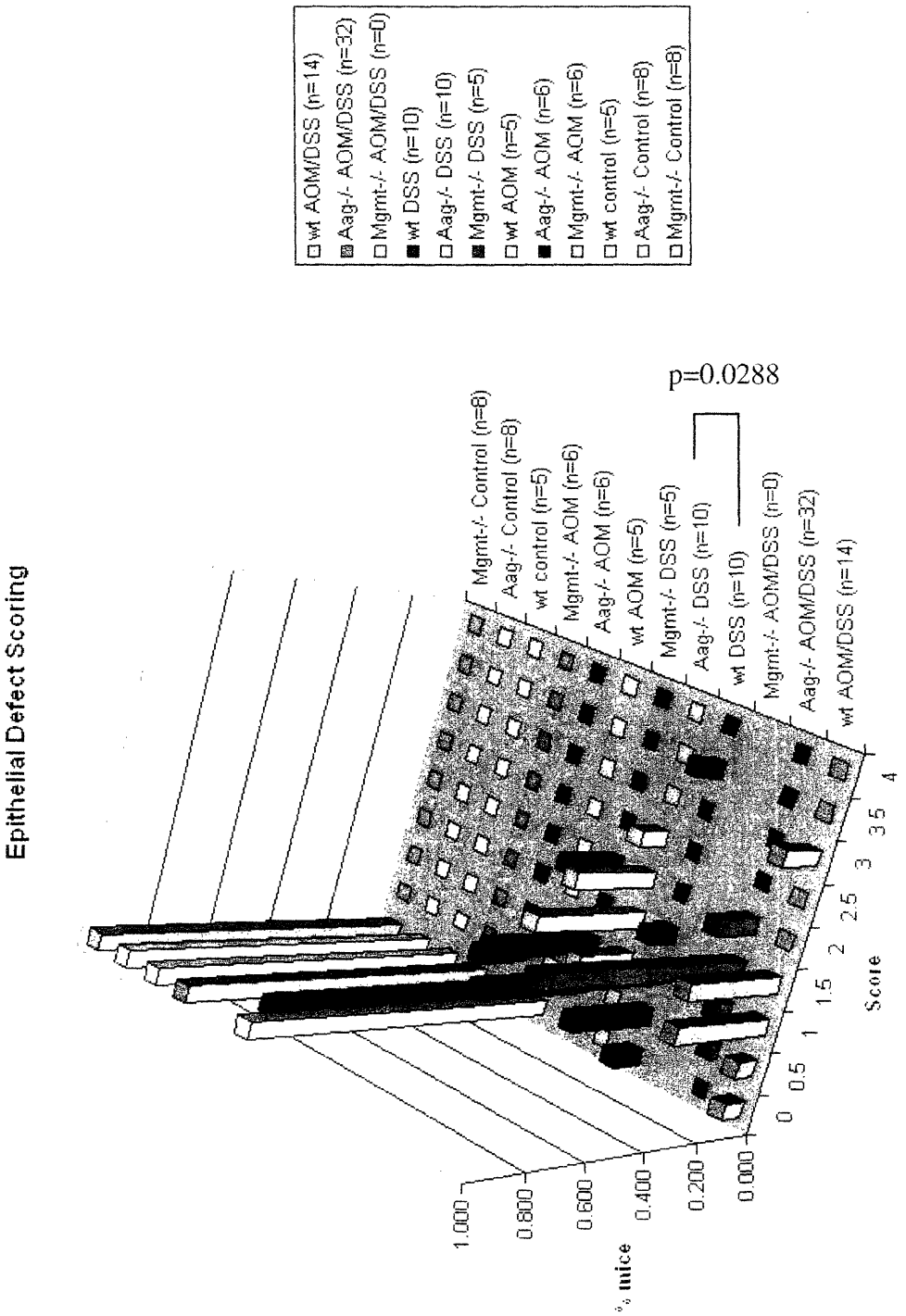

Figure 29. Epithelial Defect scoring. There is a significant difference in score between *Aag*$^{-/-}$ and wild type mice treated with DSS.

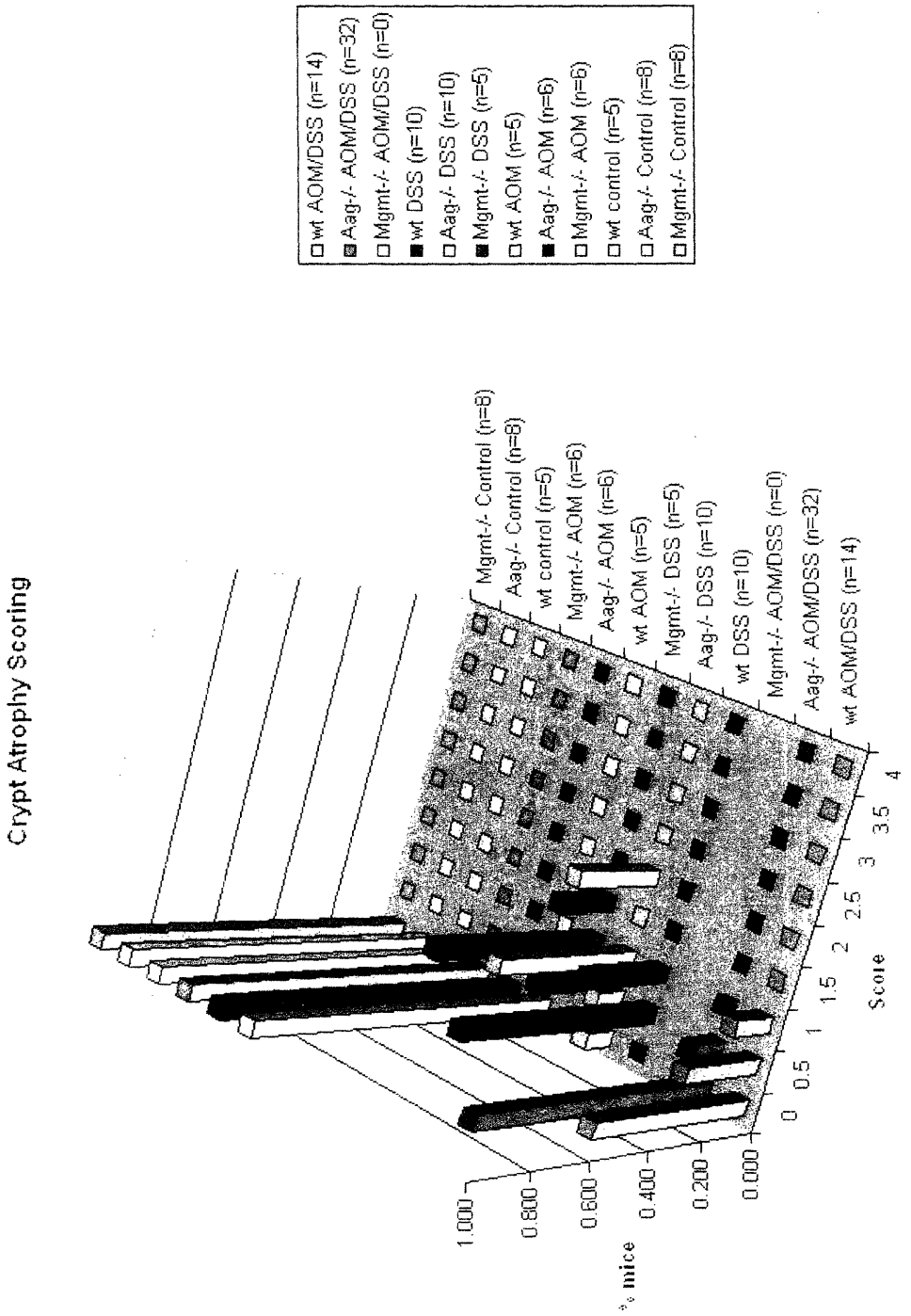

Figure 30. Crypt Atrophy scoring. There are no significant differences among treatment groups.

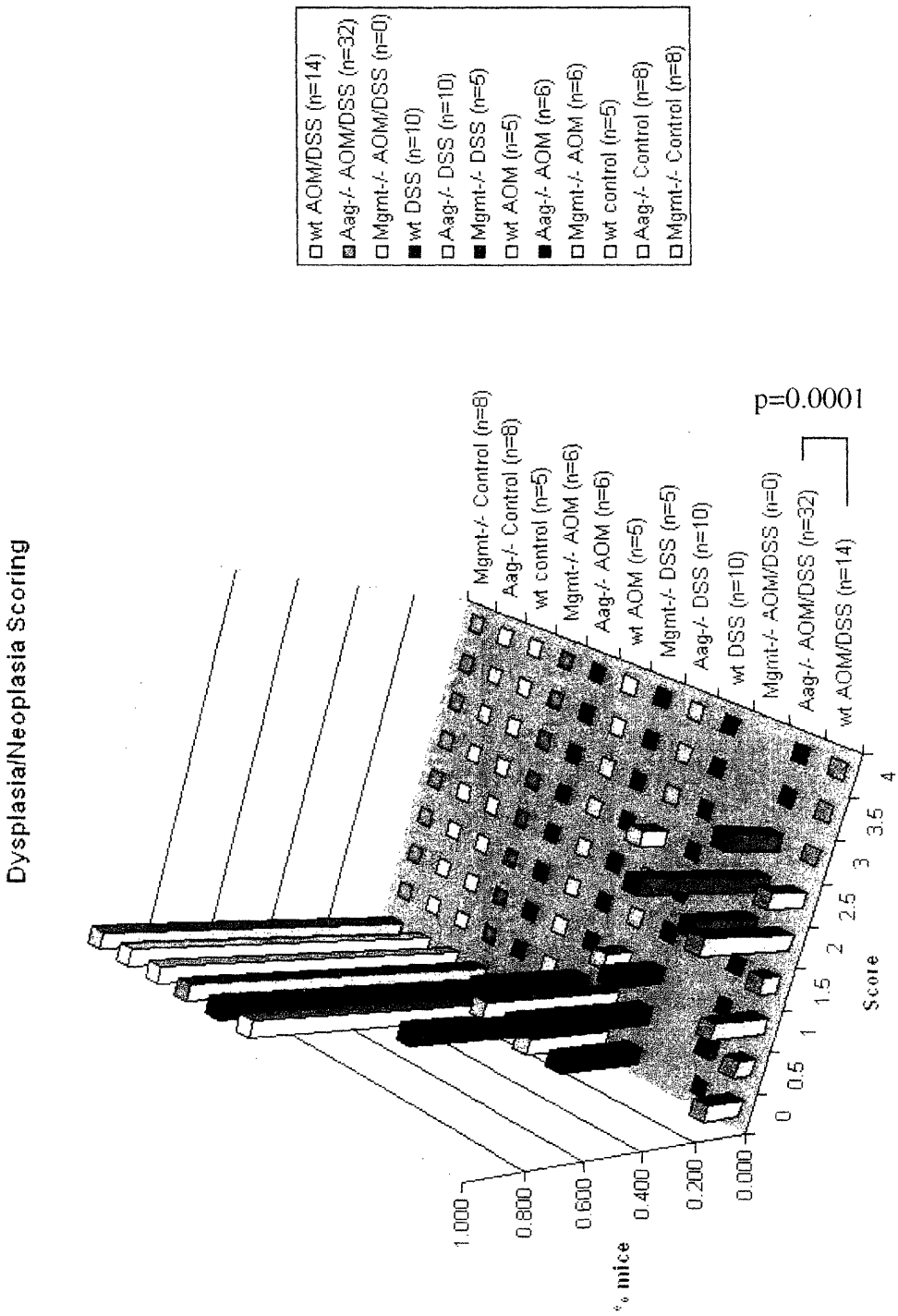

Figure 31. Dysplasia/Neoplasia scoring. There is a significant difference in score between *Aag*$^{-/-}$ and wild type mice treated with AOM and DSS.

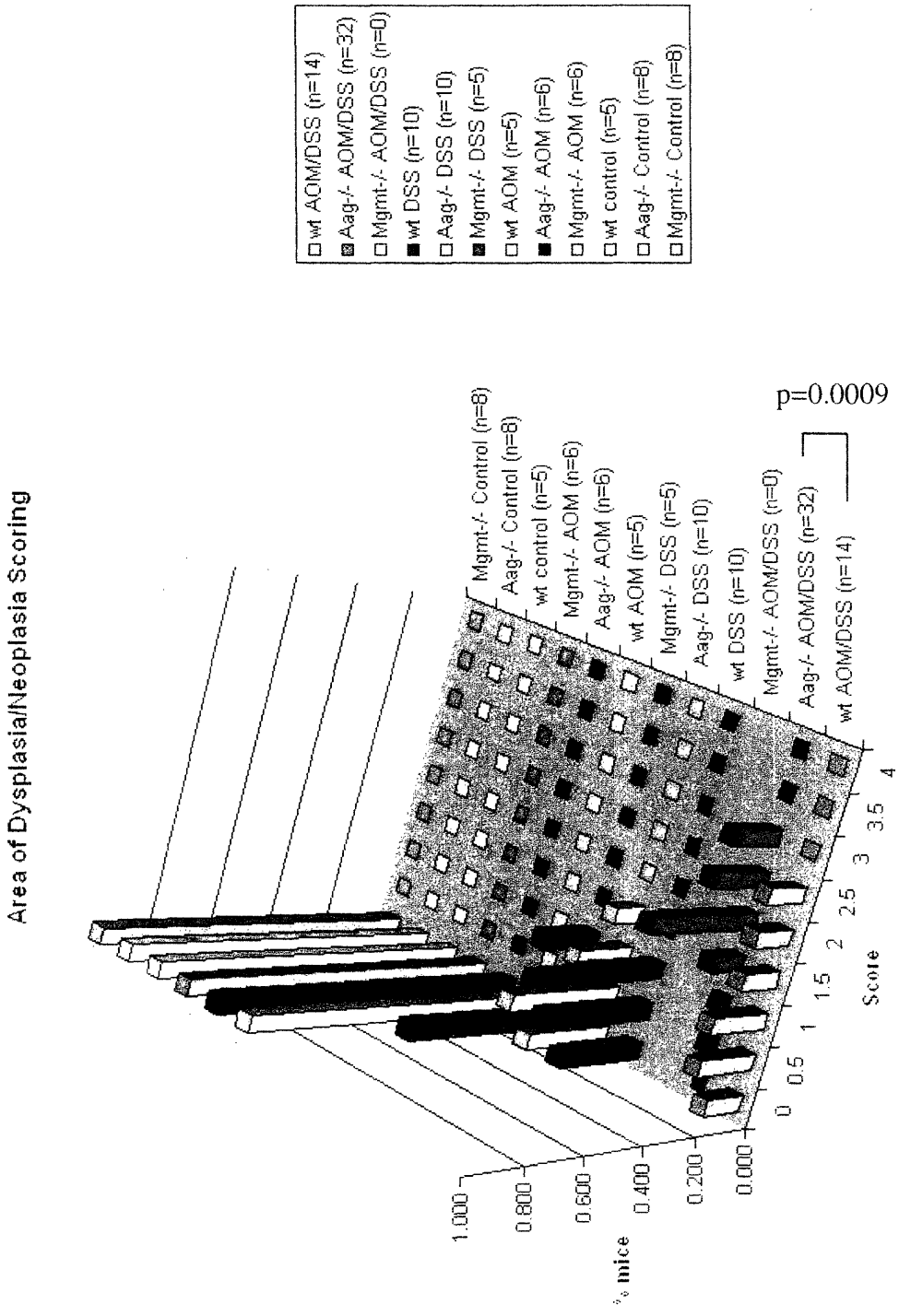

Figure 32. Area of Dysplasia/Neoplasia scoring. There is a significant difference in score between *Aag*$^{-/-}$ and wild type mice treated with AOM and DSS.

Chapter 4: Discussion

Since there was first thought to be a link between inflammation and cancer, many groups have tried and made progress toward understanding the process which bonds the two. As there is no cure for IBD, and it is difficult to monitor IBD patients for cancer, understanding inflammation and its contribution to cancer development is very important. As previously stated, risk of colorectal cancer increases at a rate of 0.5-1.0% per year after 7 years of colitis.[5] The severity of these diseases calls for better ability to monitor and treat them.

In both UC and CD, there are increased levels of εA, εG, εC in the DNA of affected tissues.[3] Also, 3-methyladenine DNA glycosylase shows adaptively increasing activity in response to increasing inflammation in UC colon epithelium.[4] This suggests that *AAG* plays a very important role in inflammation leading to cancer. 3-methyladenine DNA glycosylases may protect against mutagens and cytotoxicity due to environmental or chemical agents by removing alkylated bases or may have detrimental effects by leaving too many abasic sites.[6] If a UC patient had a deficiency in 3-methyladenine-DNA-glycosylase activity, they may be more susceptible to mutations and cancer if they are unable to repair the DNA damage caused by inflammatory cytokines and RONS. It has been shown through the results of the described experiments that lack of the *Aag* gene in mice leads to the development of a significantly greater number of polyps during chemically induced IBD.

Mouse models are able to give insight into the possible mechanisms of a disease and can closely simulate human response to sicknesses. Using, the AOM and DSS model of colitis, the importance of the BER response pathway has been shown in the case of chronic inflammation. Removal of *Aag*, which initiates BER, was found to cause sensitivity in mice treated with AOM and DSS, and is the first phenotype of sensitivity to an agent documented for this animal model. The DSS/AOM is highly reproducible, which can be seen by the small error bars for all results shown above. Multiple cycles of DSS induce chronic inflammation which is very relevant to human disease.

The aims of this project were to determine the consequences of chronic inflammation due to IBD, modulated by the absence of *Aag* substrate repair, to determine pathological differences given chronic inflammation and a tumor initiation event, modulated by the absence of *Aag* substrate repair, and to determine if differences in pathology were due to accumulation of DNA lesions or inherent differences in inflammatory processes in 3-methyladenine-DNA-glycosylase deficient ($Aag^{-/-}$) mice.

When treated with DSS, $Aag^{-/-}$ mice were found to have signs of increased disease when compared to wild type. The results of this experiment showed that there was no difference in polyp formation between the two genotypes, however, colon length and spleen weight results indicate more severe disease in the $Aag^{-/-}$ mice. Both animal types showed a decrease in colon length, which is an indication of healing ulcers and fistulas, and $Aag^{-/-}$ animals showed a large increase in spleen weight compared to wild type which only showed a slight increase. The $Aag^{-/-}$ mice showed a 2.7 cm decrease in colon length

whereas the wild type animals showed only a 0.4 cm decrease in length. Also, spleen weight was about 0.6% of body weight in *Aag*$^{-/-}$ treated animals and was only about 0.3% in wild type treated animals, and about 0.3% in controls, so wild type spleens do not seem to have been affected much by DSS treatment while *Aag*$^{-/-}$ spleens became enlarged.

When treated with AOM, which acts as a tumor initiator, and DSS, it was found that AOM causes some background changes, but that effects of DSS are greatly amplified. With AOM alone, there was no tumor formation in wild type or *Aag*$^{-/-}$ animals, but with the addition of DSS, the average number of polyps was about 8 tumors per mouse in the wild type and about 22 tumors per mouse in the *Aag*$^{-/-}$ corresponding to a 2.95 fold increase. This suggests that a single initiation event is not enough to cause tumor formation, and chronic inflammation is necessary to promote tumor development. The size and type of tumors appeared to be similar between the two animal types and all animals, regardless of genotype, formed tumors.

With AOM alone, colon length decreased 1 cm in *Aag*$^{-/-}$ animals and increased 1.1 cm in wild type animals. This indicates that AOM has a slight negative effect on *Aag*$^{-/-}$ animals compared to wild type. With AOM and DSS treatment, colon length decreased 2.5 cm in *Aag*$^{-/-}$ and 0.8 cm in wild type animals. This result is similar to results of DSS alone, which means that the decrease in colon length is mainly a result of inflammation.

Spleen weight was found to be 0.4 % of body weight in *Aag*$^{-/-}$ animals and 0.3 % of body weight in wild type treated only with AOM. Again wild type spleens do not seem to have been affected much by DSS treatment while *Aag*$^{-/-}$ spleens became slightly enlarged. However, when DSS treatment was added, spleen weight increased to 0.8 % of body weight in *Aag*$^{-/-}$ animals and 0.6 % of body weight in wild type animals. The spleen is involved in the production and maintenance of red blood cells, the production of some white blood cells, and is a part of the lymph and immune systems. It makes sense that the spleen would enlarge due to a severe immune response and the rectal bleeding caused by DSS treatment. In general, the AOM seems to have a modest effect on the *Aag*$^{-/-}$ animals, but when treated with DSS, the differences between wild type and *Aag*$^{-/-}$ animals are dramatically increased.

In order to determine how applicable this result would be to human IBD patients, it is important to determine if differences seen in *Aag*$^{-/-}$ animals are due to the accumulation of damaged DNA bases, or some inherent difference in the inflammatory process in these mice. Mice would be treated for a short period of time with DSS and ideally inflammatory response and DNA lesions would be measured over a period of time to examine the healing process in both animals.

Chapter 5: *Mgmt* Results

Unlike *Aag*$^{-/-}$ mice, there have been previously reported phenotypes in *Mgmt*$^{-/-}$ mice treated with damaging agents. It is still interesting, however, to study the role of *Mgmt* in chronic inflammation and cancer, as *Mgmt* has been known to protect against alkylation damage in some cases. *Mgmt* participates in the repair of both damage induced by chronic inflammation and damage induced by AOM. As with *Aag*, there was rationale for thinking that *Mgmt*$^{-/-}$ mice would show a phenotype when treated chronically with DSS.

Mgmt$^{-/-}$ mice were treated along with the wild type and *Aag*$^{-/-}$ mice to determine the consequences of chronic inflammation due to IBD, modulated by the absence of O^6MeG repair. Signs of increased disease, such as spleen weight, body weight, and colon length, were measured in this experiment. Since about 5% of patients with colitis go on to develop colon cancer, mouse intestines were also visually inspected for polyp formation, and any polyps were counted using a stereomicroscope.

All *Mgmt*$^{-/-}$ mice treated with AOM plus DSS died after the first week of DSS treatment. This was likely due to many factors including blood loss, dehydration, and decreased food intake. In terms of polyp formation, no polyps were found in *Mgmt*$^{-/-}$ mice treated with DSS alone, however polyp multiplicity in *Mgmt*$^{-/-}$ mice treated with AOM alone was found to be 0.83 ± 1.17 (Figure 33) with an incidence of 0.5 (Figure 34). This seems to suggest that the damage induced by chronic inflammation alone that is repaired by *Mgmt*

is not enough to cause the formation of polyps; however the damage induced by AOM causes polyp formation where none developed in wild type or *Aag*$^{-/-}$ mice.

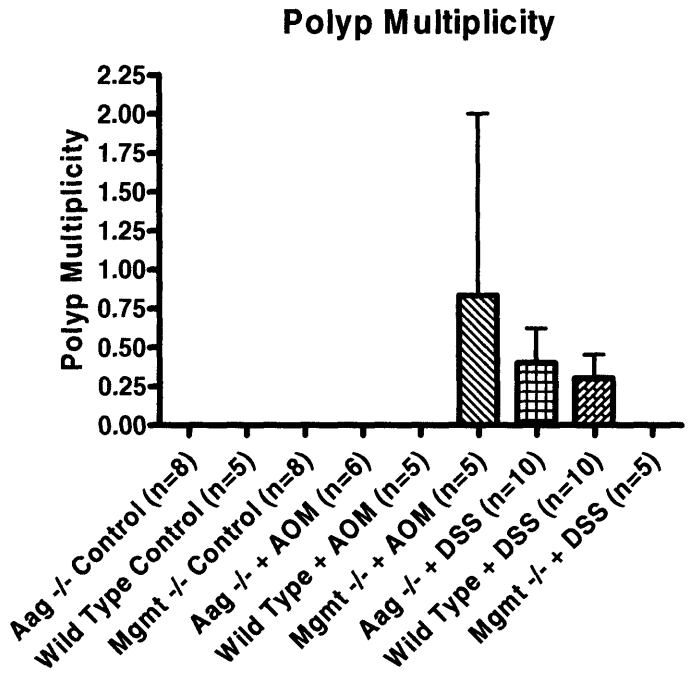

Figure 33. This figure shows that there were no polyps found in *Mgmt*$^{-/-}$ mice treated with DSS alone. There were polyps found in *Mgmt*$^{-/-}$ mice treated with AOM alone, but not in wild type or *Aag*$^{-/-}$ mice. *Aag*$^{-/-}$ and Wild Type DSS data is from Figure 10. *Aag*$^{-/-}$ and Wild Type AOM data is from Figure 17.

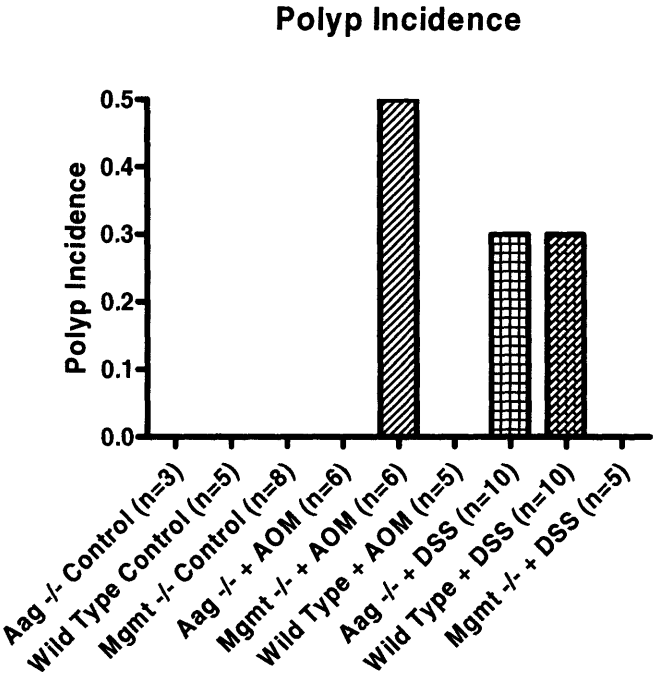

Figure 34. This figure shows that there were no polyps found in *Mgmt*$^{-/-}$ mice treated with DSS alone, but there were polyps found in half of the *Mgmt*$^{-/-}$ mice treated with AOM alone. *Aag*$^{-/-}$ and Wild Type DSS data is from Figure 11. *Aag*$^{-/-}$ and Wild Type AOM data is from Figure 18.

In addition to polyp incidence and multiplicity, colon length was measured. Changes in colon length for *Mgmt*$^{-/-}$ mice were approximately the same as *Aag*$^{-/-}$ mice when treated with AOM alone and DSS alone (Figures 35 and 36). This suggests that although there was a similar amount of healing in *Mgmt*$^{-/-}$ mouse colons compared to *Aag*$^{-/-}$ mice, the *Mgmt*$^{-/-}$ mice did not develop polyps, even though polyps were seen in wild type mice with smaller changes in colon length. Sample numbers would need to be increased to determine whether or not *Mgmt*$^{-/-}$ mice could somehow be protecting against the

development of tumors, although pathology analysis also indicates the *Mgmt*$^{-/-}$ mice are not worse off than the wild type mice for all treatments.

Figure 35 shows a graph of colon length and Figures 36 shows a graph of change in colon length from control animals treated with DSS alone and AOM alone respectively. In *Mgmt*$^{-/-}$ animals, the average colon length of DSS treated animals was found to be 7.5 ± 1.3 cm with a change in colon length of -2.2 ± 0.7 cm. In *Mgmt*$^{-/-}$ animals, the average colon length of AOM treated animals was found to be 6.0 ± 0.6 cm with a change in colon length of -1.0 ± 0.6 cm. In *Mgmt*$^{-/-}$ untreated animals, the average colon length was found to be 8.5 ± 0.6 cm.

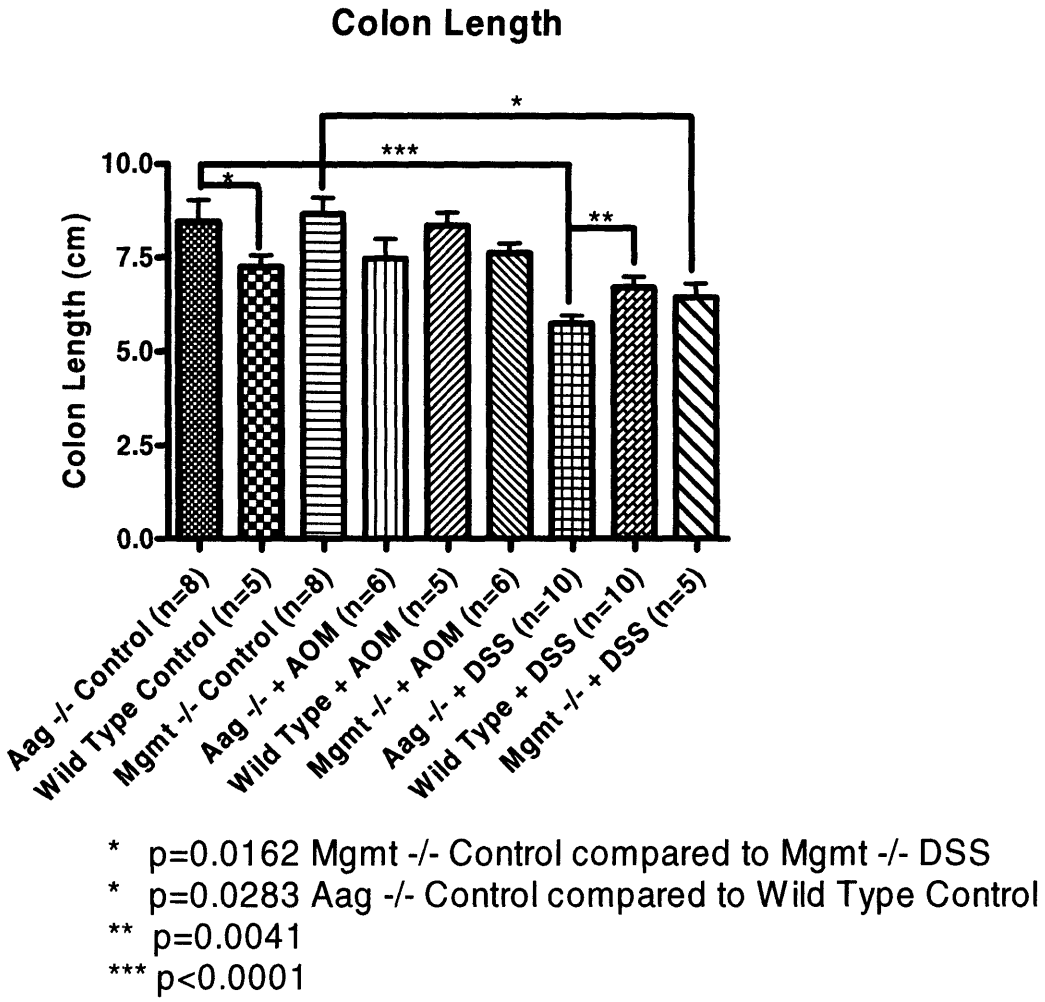

Figure 35. This figure shows colon length data for treatment with AOM alone and DSS alone. *Mgmt*$^{-/-}$ and *Aag*$^{-/-}$ mice both show a decrease in colon length from controls when treated with DSS alone. *Aag*$^{-/-}$ and Wild Type DSS data is from Figure 13. *Aag*$^{-/-}$ and Wild Type AOM data is from Figure 20.

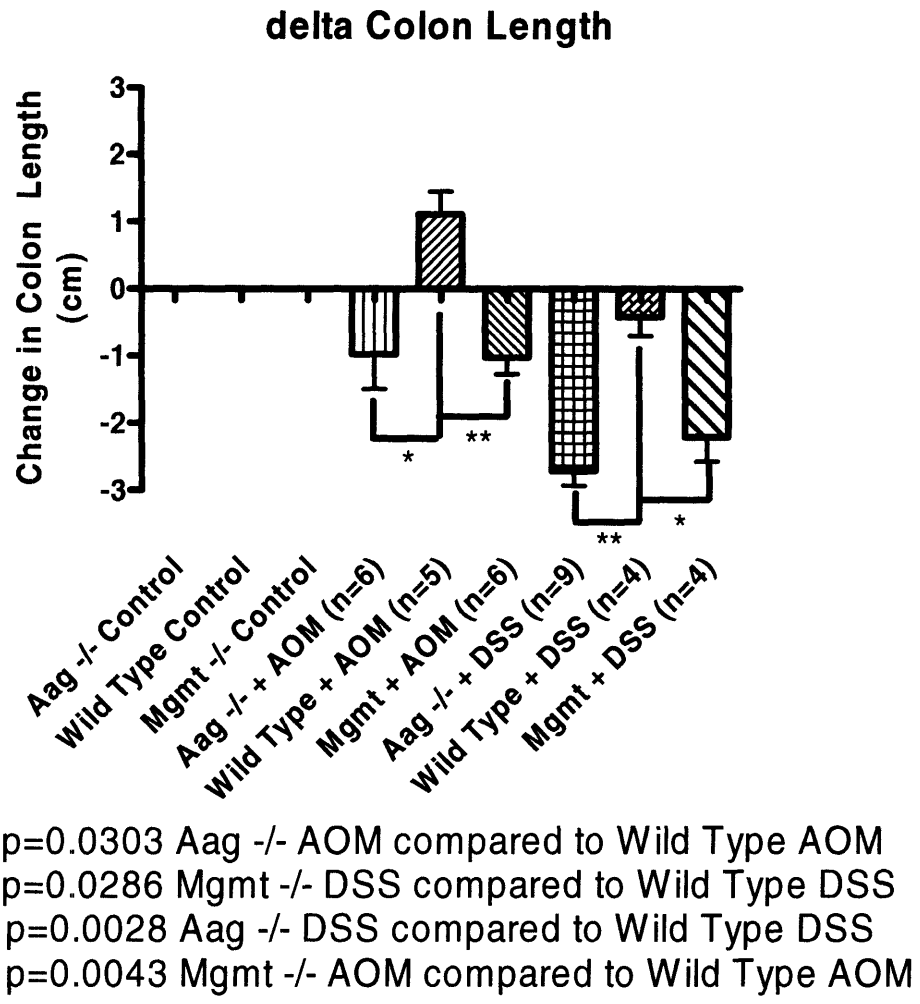

Figure 36. This figure shows that *Mgmt*$^{-/-}$ mice show a similar change in colon length to *Aag*$^{-/-}$ mice treated with DSS alone or AOM alone. *Aag*$^{-/-}$ and Wild Type DSS data is from Figure 14. *Aag*$^{-/-}$ and Wild Type AOM data is from Figure 21.

In addition to colon length, spleen and body weights also indicated that response of *Mgmt*$^{-/-}$ mice to AOM alone and DSS alone were similar to that of *Aag*$^{-/-}$ mice, even though polyp formation results differed. Figure 37 shows spleen weight as a percent of final body weight and Figure 38 shows body weight results as percent change in body weight from the animals' original body weight.

In *Mgmt*$^{-/-}$ animals, the average spleen weight of DSS treated animals was found to be 0.45 ± 0.05 % of final body weight. In *Mgmt*$^{-/-}$ animals, the average spleen weight of AOM treated animals was found to be 0.36 ± 0.06 % of final body weight. In *Mgmt*$^{-/-}$ untreated animals, the average spleen weight was found to be 0.36 ± 0.08 % of final body weight. Changes in body weight of *Mgmt*$^{-/-}$ mice treated with DSS alone were in between wild type and *Aag*$^{-/-}$ weights, and changes in body weight of *Mgmt*$^{-/-}$ mice treated with AOM alone were similar to *Aag*$^{-/-}$ weights.

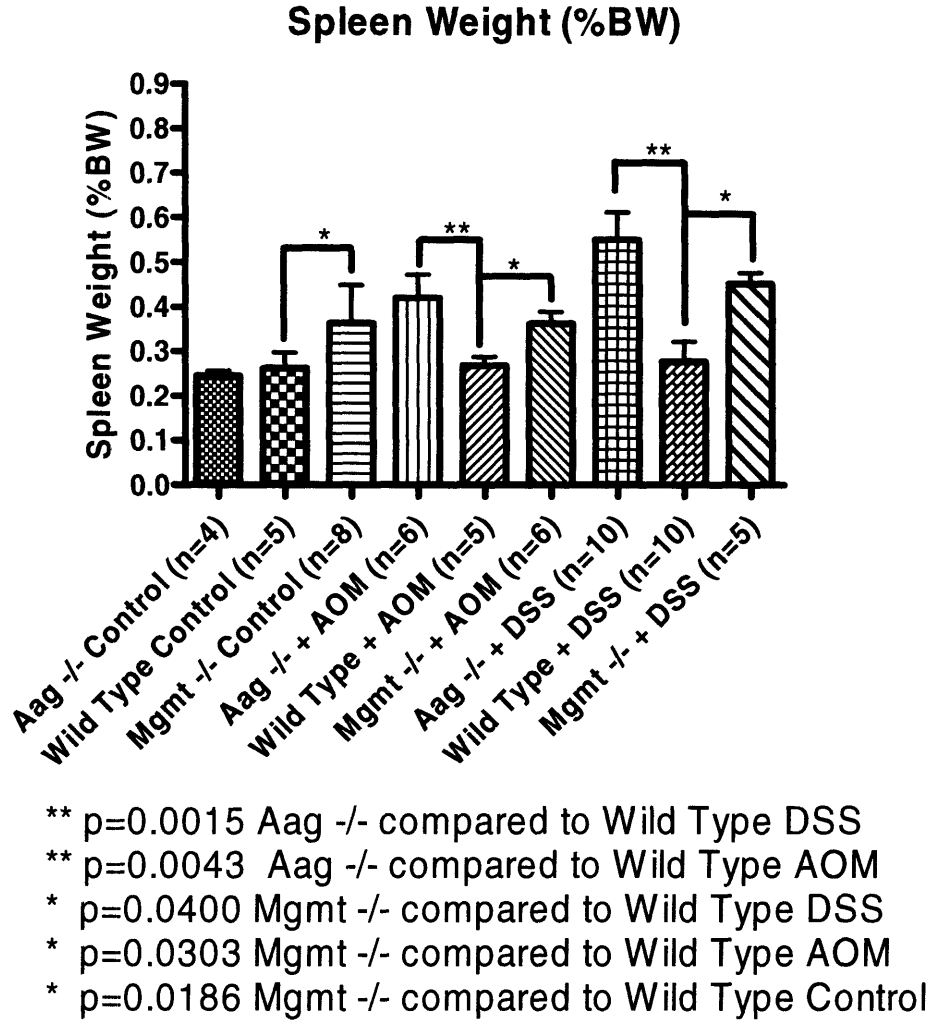

Figure 37. This figure shows that spleen weight for *Mgmt*$^{-/-}$ mice treated with DSS alone or AOM alone are significantly different than that of wild type mice. *Aag*$^{-/-}$ and Wild Type DSS data is from Figure 15. *Aag*$^{-/-}$ and Wild Type AOM data is from Figure 22.

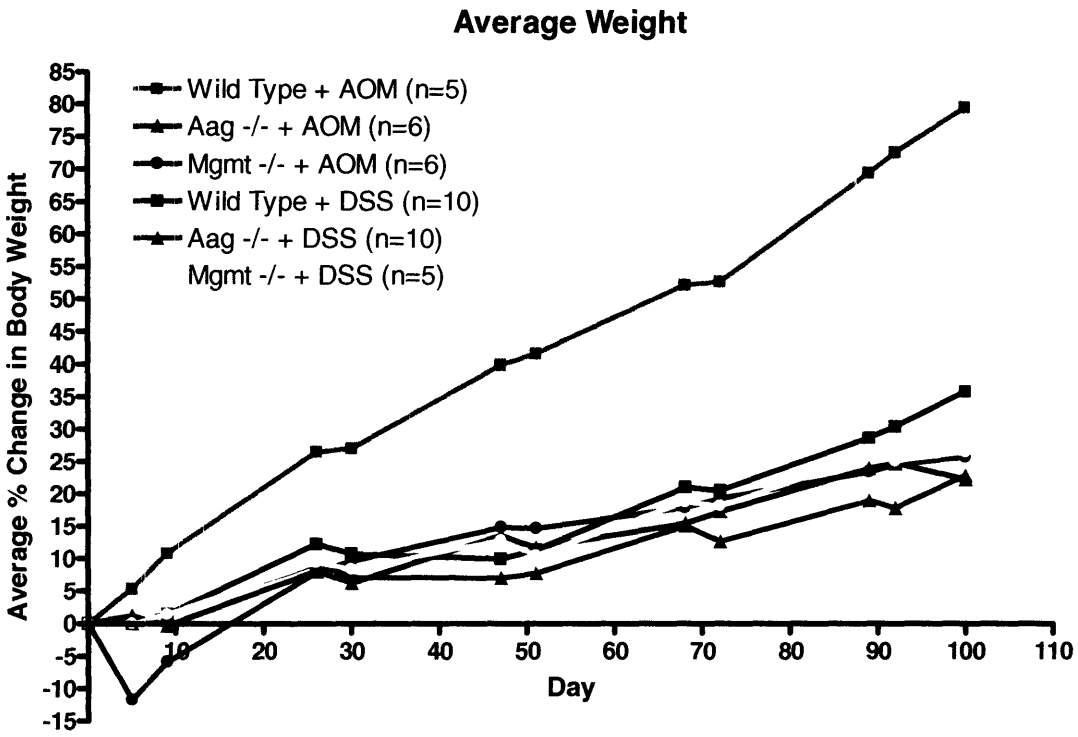

Figure 38. This figure shows that there *Mgmt*$^{-/-}$ mice showed body weights between those of wild type and *Aag*$^{-/-}$ mice when treated with AOM alone and DSS alone. *Aag*$^{-/-}$ and Wild Type DSS data is from Figure 16. *Aag*$^{-/-}$ and Wild Type AOM data is from Figure 23.

Although *Mgmt*$^{-/-}$ mice showed similar phenotype to *Aag*$^{-/-}$ in terms of colon length, spleen weight, and body weight when treated with AOM alone and DSS alone, there was definitely a difference in the responses, which can be seen in the polyp results and also by the death of the *Mgmt*$^{-/-}$ animals when treated with both drugs. The two animal types had opposite responses in terms of polyp formation. *Aag*$^{-/-}$ animals developed polyps with DSS alone whereas *Mgmt*$^{-/-}$ animals did not, and *Mgmt*$^{-/-}$ mice developed polyps with AOM alone whereas *Aag*$^{-/-}$ mice did not. This is a very interesting finding, which should be further confirmed and studied.

Conclusions and Future Experiments

Previously, there have been no reported phenotypes for *Aag*$^{-/-}$ mice treated with damaging agents. A phenotype is important because it can allow a model to be used for determining the role of a particular gene or the effect of a treatment for disease. It was postulated that *Aag*$^{-/-}$ mice might show a phenotype when treated chronically with DSS since *Aag* plays such an important role in the repair of DNA damage induced by chronic inflammation.

Signs of increased disease, such as spleen weight, body weight, and colon length, were measured in this experiment. Since about 5% of patients with colitis go on to develop colon cancer, polyp formation was also used as an indicator of disease. Results indicate that for treatment with DSS alone, there is no significant difference in the polyp formation between wild type and *Aag*$^{-/-}$ animals. *Aag*$^{-/-}$ mice, however, did not form any polyps, whereas *Aag*$^{-/-}$ and wild type mice both had a polyp incidence of 0.3. The fact that both *Aag*$^{-/-}$ and wild type mice developed polyps confirms that DSS acts as both an initiator and a promoter in these two animal types. It is not yet clear why DSS does not act similarly in *Mgmt*$^{-/-}$ mice. Although there were not significant differences in polyp multiplicity or incidence between wild type and *Aag*$^{-/-}$ mice, there was found to be a significant difference in epithelial defects, change in colon length, and spleen weight. These are indications of more severe disease and in the *Aag*$^{-/-}$ animals and give the first phenotype to be described for *Aag*$^{-/-}$ animals treated with a damaging agent.

These results are extremely encouraging and motivate further study of the role of *Aag* in inflammation and cancer. In order to determine if *Aag*$^{-/-}$ animals would have an increased tumor response compared to wild type given initial damage, animals were treated with a tumor initiation agent prior to inducing chronic inflammation. Given the results of the above, it is clear that *Aag* is contributing to prevention of the harmful effects of chronic inflammation. It was formerly unclear whether or not the deletion of *Aag* would lead to sensitivity or resistance in the whole animal model since previous results for other DNA repair knockouts have been surprising. Although it is interesting to see a phenotype from DSS treatment alone, the initial aim of this project was in studying inflammation and cancer, as many IBD patients go on to develop colorectal cancer.

Although no significant differences in polyps were seen with DSS treatment alone, there were indications of increased disease. It was therefore be expected that *Aag*$^{-/-}$ mice treated with a tumor initiator would show some difference in polyp multiplicity and incidence under chronic inflammation conditions due to the lack of *Aag* substrate repair. With the addition of AOM, *Aag*$^{-/-}$ mice indeed show a significant increase in tumor multiplicity.

Aag$^{-/-}$ animals, were found to have a polyp multiplicity 2.95 times greater than wild type with a p-value less than 0.0001. In addition, spleen weight was increased and colon length was decreased. There were also significant increases in dysplasia/neoplasia and area of dysplasia/neoplasia in *Aag*$^{-/-}$ mice treated with both AOM and DSS. The results of this experiment show that there is a significant difference in the wild type and *Aag*$^{-/-}$

animals' response to chronic inflammation with a tumor initiation event. Again, this is the first phenotype to be seen in *Aag*$^{-/-}$ mice, and is extremely encouraging because of the large difference in polyp multiplicity.

Mgmt$^{-/-}$ mice did not survive treatment with AOM plus DSS, however went on to develop polyps when treated with AOM alone. Although *Mgmt*$^{-/-}$ mice showed similar phenotype to *Aag*$^{-/-}$ mice in terms of colon length, spleen weight, and body weight when treated with AOM alone and DSS alone, the two animal types had opposite responses in terms of polyp formation. *Aag*$^{-/-}$ animals developed polyps with DSS alone whereas *Mgmt*$^{-/-}$ animals did not, and *Mgmt*$^{-/-}$ mice developed polyps with AOM alone whereas *Aag*$^{-/-}$ mice did not. This is a very interesting finding, which should be confirmed and further studied.

It has been determined that 3-methyladenine DNA glycosylase and the BER pathway are important in protecting against the effects of chronic inflammation. In a future study, it would be very beneficial to determine if transgenic *Aag* over-expresser mice protect against the damage induced by chronic inflammation. This would make intestinal gene therapy a possible approach to finding the first cure for IBD and inflammation associated colorectal cancer.

Other genotypes could also be used to determine the effects of relevant pathways in linking inflammation and cancer. Future experiments would also include development of a better model, which shows closer relevance to human IBD and can be used to test

therapies. A start would be to test longer cycles of DSS to see if polyps would progress to cancer. It would also be worth looking in to gender effects, as literature shows males to be more susceptible to AOM induced tumors. In this experiment, there is not enough data to determine if there is gender specific susceptibility due to DSS alone.

There is much work to be done to understand the link between chronic inflammation and cancer, however there have been many experiments which have elucidated various pieces of the puzzle. Hopefully in the near future, scientists will be able to piece this newly discovered information together and find a better treatment or cure for IBD and inflammation associated colorectal cancer.

References

1. **Suzuki, R., et al., *Sequential observations on the occurrence of preneoplastic and neoplastic lesions in mouse colon treated with azoxymethane and dextran sodium sulfate.* Cancer Science, 2004. 95(9): p. 721-727.**

2. **Tanaka, T., et al., *A novel inflammation-related mouse colon carcinogenesis model induced by azoxymethane and dextran sodium sulfate.* Cancer Science, 2003. 94(11): p. 965-973.**

3. **Bartsch, H. and J. Nair, *Potential role of lipid peroxidation derived DNA damage in human colon carcinogenesis: studies on exocyclic base adducts as stable oxidative stress markers.* Cancer Detection and Prevention, 2002. 26: p. 308-312.**

4. **Hofseth, L.J., et al., *The adaptive imbalance in base excision-repair enzymes generates microsatellite instability in chronic inflammation.* The Journal of Clinical Investigation, 2003. 112(12): p. 1887-1894.**

5. **Itzkowitz, S.H. and X. Yio, *Inflammation and Cancer IV. Colorectal cancer in inflammatory bowel disease: the role of inflammation.* American Journal of Physiology - Gastrointestinal and Liver Physiology, 2004. 287: p. G7-G17.**

6. **Wyatt, M.D., et al., *3-Methyladenine DNA glycosylases: structure, function, and biological importance.* BioEssays, 1999. 21: p. 668-676.**

7. **MayoClinic, *Ulcerative Colitis*.** Retrieved from, http://www.mayoclinic.org/ulcerative-colitis/details.html

8. **Greten, F.R., et al., *IKKβ links inflammation and tumorigenesis in a mouse model of colitis-associated cancer.* Cell, 2004. 118: p. 285-296.**

9. **Gillen, C., et al., *Ulcerative colitis and Crohn's disease: a comparison of the colorectal cancer risk in extensive colitis.* Gut, 1994. 35(11): p. 1507-1508.**

10. **Okayasu, I., et al., *Dysplasia and carcinoma development in a repeated dextran sulfate sodium-induced colitis model.* Journal of Gastroenterology and Hepatology, 2002. 17: p. 1078-1083.**

11. **eMedicine, *Colitis: Exams and Tests*.** Retrieved from, http://www.emedicinehealth.com/articles/5868-5.asp

12. **Rutter, M., et al., *Severity of inflammation is a risk factor for colorectal neoplasia in ulcerative colitis.* Gastroenterology, 2004. 126(2): p. 451-459.**

13. **Lodish, H., et al., *Molecular Cell Biology*. 2004, New York, NY: W.H. Freeman and Company.**

14. **Fuji, S., et al., *Development of colonic neoplasia in p53 deficient mice with experimental colitis induced by dextran sulphate sodium.* Gut, 2004. 53: p. 710-716.**

15. **Kawai, N., et al., *Tumor Necrosis Factor α Stimulates Invasion of Src-Activated Intestinal Cells.* Gastroenterology, 2002. 122(3): p. 331-339.**

16. **Singer, I., et al., *Expression of inducible nitric oxide synthase and nitrotyrosine in colonic epithelium in inflammatory bowel disease.* Gastroenterology, 1996. 111(4): p. 871-875.**

17. **Wiseman, H. and B. Halliwell, *Damage to DNA by reactive oxygen and nitrogen species: role in inflammatory disease and progression to cancer.* Biochemical Journal, 1996. 313: p. 17-29.**

18. **Kelly, M.R., *DNA Repair*. 2004: Indianapolis.** Retrieved March 1, 2005, from, http://cmg.iupui.edu/G865/KelleyG865_DNA_repair_lectures2004.pdf

19. **Glassner, B.J., et al., *DNA repair methyltransferase (Mgmt) knockout mice are sensitive to the lethal effects of chemotherapeutic alkylating agents.* Mutagenesis, 1999. 14(3): p. 339-347.**

20. **Engelward, B.P., et al., *Base excision repair deficient mice lacking the Aag alkyladenine DNA glycosylase.* PNAS, 1997. 94: p. 13087–13092.**

21. **Hoffman, J.C., et al., *Animal Models of Inflammatory Bowel Disease: An Overview.* Pathobiology, 2002/2003. 70(3): p. 121-130.**

22. **Kitajima, S., S. Takuma, and M. Morimoto, *Tissue distribution of dextran sulfate sodium (DSS) in the acute phase of murine DSS-induced colitis.* Journal of Vetinary Medical Science, 1999. 61(1): p. 67-70.**

23. **CancerWEB, *Online Medical Dictionary*.**

24. **Strober, W., I.J. Fuss, and R.S. Blumberg, *The immunology of mucosal models of inflammation.* Annual Review of Immunology, 2002. 20: p. 495-549.**

25. **Nambiar, P.R., et al., *Preliminary analysis of azoxymethane induced colon tumors in inbred mice commonly used as transgenic/knockout progenitors.* International Journal of Oncology, 2003. 22: p. 145-150.**

26. **Suzuki, R., et al., *Dose-dependent promoting effect of dextran sodium sulfate on mouse colon carcinogenesis initiated with azoxymethane.* Histology and Histopathology, 2005. 20: p. 483-492.**

27. **Suzuki, R., et al., *Strain differences in the susceptibility to azoxymethane and dextran sodium sulfate-induced colon carcinogenesis in mice.* Carcinogenesis, 2005.**